AD_____

Award Number: DAMD17-98-1-8251

TITLE: Understanding the Role of Replication Protein A and RAD52 in Breast Cancer

PRINCIPAL INVESTIGATOR: Gloria E. Borgstahl, Ph.D.

CONTRACTING ORGANIZATION: The University of Toledo
Toledo, Ohio   43606-3390

REPORT DATE: October 2002

TYPE OF REPORT: Annual

PREPARED FOR: U.S. Army Medical Research and Materiel Command
Fort Detrick, Maryland 21702-5012

DISTRIBUTION STATEMENT: Approved for Public Release;
Distribution Unlimited

The views, opinions and/or findings contained in this report are those of the author(s) and should not be construed as an official Department of the Army position, policy or decision unless so designated by other documentation.

20030513 105

REPORT DOCUMENTATION PAGE

Public reporting burden for this collection of information is estimated to average 1 hour per response, including the time for reviewing instructions, searching existing data sources, gathering and maintaining the data needed, and completing and reviewing this collection of information. Send comments regarding this burden estimate or any other aspect of this collection of information, including suggestions for reducing this burden to Washington Headquarters Services, Directorate for Information Operations and Reports, 1215 Jefferson Davis Highway, Suite 1204, Arlington, VA 22202-4302, and to the Office of Management and Budget, Paperwork Reduction Project (0704-0188), Washington, DC 20503

1. AGENCY USE ONLY (Leave blank)	2. REPORT DATE October 2002	3. REPORT TYPE AND DATES COVERED Annual (25 Sep 01 - 24 Sep 02)

4. TITLE AND SUBTITLE
Understanding the Role of Replication Protein A and RAD52 in Breast Cancer

5. FUNDING NUMBERS
DAMD17-98-1-8251

6. AUTHOR(S):
Gloria E. Borgstahl, Ph.D.

7. PERFORMING ORGANIZATION NAME(S) AND ADDRESS(ES)

The University of Toledo
Toledo, Ohio 43606-3390

E-MAIL:
gborgst@unmc.edu

8. PERFORMING ORGANIZATION REPORT NUMBER

9. SPONSORING / MONITORING AGENCY NAME(S) AND ADDRESS(ES)

U.S. Army Medical Research and Materiel Command
Fort Detrick, Maryland 21702-5012

10. SPONSORING / MONITORING AGENCY REPORT NUMBER

11. SUPPLEMENTARY NOTES
Original contains color plates: All DTIC reproductions will be in black and white.

12a. DISTRIBUTION / AVAILABILITY STATEMENT
Approved for Public Release; Distribution Unlimited

12b. DISTRIBUTION CODE

13. ABSTRACT (Maximum 200 Words)
This research focuses on structural studies of human replication protein A (RPA) and RAD52 in recombination-based repair of double-stranded DNA breaks. This DNA repair pathway has been directly linked to breast cancer through BRCA1 and BRCA2 protein-protein interactions. Also, mutations in the ataxia telangiectasia (AT) gene are implicated in breast cancer and recently AT kinase was shown to phosphorylate the N-terminus of the 32 kDa subunit of RPA. The goals of the Borgstahl laboratory are to understand the role of RPA phosphorylation and RPA/RAD52 protein-protein interactions in DNA repair. The ultimate goal of this research is to provide an understanding of this process at the atomic level.

14. SUBJECT TERMS
breast cancer

15. NUMBER OF PAGES
30

16. PRICE CODE

17. SECURITY CLASSIFICATION OF REPORT Unclassified	18. SECURITY CLASSIFICATION OF THIS PAGE Unclassified	19. SECURITY CLASSIFICATION OF ABSTRACT Unclassified	20. LIMITATION OF ABSTRACT Unlimited

Table of Contents

1. Abstract for poster presentation: W. Ranatunga, D. Jackson and G. E. O. Borgstahl "Temperature Modulates the Higher-ordered Self-association of Rad52", Era of Hope Meeting, Orlando, Florida, September, 2002.

2. Abstract for poster presentation: D. Jackson, K. Dhar, M. Wold and G. E. O. Borgstahl "Analysis of the Rad52/RPA Complex: Evidence for Crosstalk Between RPA32, RPA70, Rad52 and ssDNA", Era of Hope Meeting, Orlando, Florida, September, 2002.

3. Reprint of publication: D. Jackson, K. Dhar, J. K. Wahl, M. S. Wold and G. E. O. Borgstahl, G. E. O. "Analysis of the Rad52/RPA Complex: Evidence for Crosstalk Between RPA32, RPA70, Rad52 and ssDNA" *J. Mol. Biol.* **321**, 133-148 (2002).

Introduction

This is the fourth annual report for Career Development Award (CDA) and IDEA award. These two awards have been combined under one award number (DAMD17-98-1-8251) and this report describes the progress made for both awards. A no-cost extension was issued October 2002; therefore an annual report is being submitted rather than a final report.

Career Development

I am grateful to the BCRP and the CDA award which has made a tremendous difference in my career. Upon the award of the CDA the chair of the Chemistry department at the University of Toledo relieved me of my formal teaching responsibilities (which constituted 40% of my effort) in order to permit me to focus my efforts on breast cancer research and to develop a breast cancer focus in my research laboratory. I continued, during the course of the year, to train graduate students. This training includes an informal special topics course in protein crystallography. Six graduate students were involved in getting this program off the ground. Three of the students (Jeff Ohren, Krishnamurthy Rajeswari and Cathy Schellert) received M.S. degrees for their efforts in the summer of 1999. Summer 2002, two doctoral students (Doba Jackson and Wasantha Ranatunga) completed their dissertations and went on to postdoctoral fellowships (at Penn State and Lawrence Berkeley National Laboratory). One other Ph.D. student (Jennifer Garlitz) is in the process of writing her dissertation and is anticipated to graduate in 2003. All students worked on various aspects of this project for their dissertation research.

Tremendous progress was made this year in the development of my career in breast cancer research. I have received two prestigious awards for this research. On April 12, 2002 I was awarded the Sigma Xi, Dion D. Raftopoulos Award for Outstanding Research and on April 26, 2002 I was awarded the University of Toledo Outstanding Research Award. This summer I served for the third time on the 2002 Army Breast Cancer study section in Molecular Biology and Genetics. I was awarded an American Cancer Society Research Scholars Grant for Beginning Investigators for four years. This year I was able to secure an exciting research intensive position in an excellent research environment to further my career in Breast Cancer research. I have recently accepted a tenured Associate Professor position at the Eppley Cancer Research Institute and moved my laboratory to the University Of Nebraska Medical Center in Omaha, NE. I resigned from the University of Toledo September 13, 2002 and the transfer of this grant to the Eppley Cancer Research Institute is in progress. My new contact information is as follows:

Dr. Gloria Borgstahl
Eppley Institute for Cancer Research
987696 Nebraska Medical Center
10732A Lied Transplant Center
Omaha, NE 68198-7696
Office (402) 559-8578
FAX (402) 559-8577

Introduction to the project

This research focuses on structural studies of human replication protein A (RPA) and RAD52. RPA is a central molecule of the molecular machinery of DNA metabolism and is essential for DNA replication, recombination and repair [15]. RPA interacts specifically with RAD52 [10] and is involved in the early stages of recombination-based repair of double-stranded DNA breaks [12]. This DNA repair pathway has been directly linked to breast cancer through BRCA1 and BRCA2 protein-protein interactions [1]. Mutations in the ataxia telangiectasia (AT) gene are also implicated in breast cancer [8] and recently AT kinase was shown to phosphorylate threonine and serine residues of the 32 kDa subunit of RPA [6]. The goals of the Borgstahl laboratory are to understand the role of RPA phosphorylation and RPA/RAD52 protein-protein interactions in DNA repair. The ultimate goal of this research is to provide an understanding of this process at the atomic level. Towards this aim constructs of RPA, RAD52 and the RPA/RAD52 complex that are suitable for crystallization will be found and then crystallized for structure determination by X-ray crystallography.

Body

Changes to the statement of work objectives from the original proposal were explained in the progress report for the period 25-Sep-98 – 24-Sep-99 and will not be repeated here. In that report objective 1 was abandoned and objective 2 was completed. Progress on objectives 3 and 4 are described in this report. The text of the objective has been copied and below each objective the tasks which have been completed are described. When appropriate any changes that have occurred are explained and how the project will proceed in the next year of this award is explained.

Objective 3: *Identify regions of RPA that interact with RAD52.*

Regions on the C-terminal domain of RPA32 and midsection of RPA70 have been identified as interacting with RAD52 in the previous reports. Recently we have found that Rad52 binding to RPA increases the ssDNA affinity of RPA. We have also found that binding by RPA disrupts the higher order self-association of Rad52. Of particular interest was the crosstalk between RPA70 and RPA32 binding to Rad52 that increase the affinity of RPA32 for ssDNA. These results have mechanistic implications in double strand break repair and together with our previously reported ELISA protein-protein interaction results were published this year. The reprint is included in the appendix: D. Jackson, K. Dhar, J. K. Wahl, M. S. Wold and G. E. O. Borgstahl, G. E. O. "Analysis of the Rad52/RPA Complex: Evidence for Crosstalk Between RPA32, RPA70, Rad52 and ssDNA" *J. Mol. Biol.* **321**, 133-148 (2002).

We also found that the RPA32 and RPA70 sites on Rad52 were separate but competitive. We determined that the RPA70 and the RPA32 sites lie within residues 218-313 of Rad52. This site will be further refined in the last year of the grant as it is anticipated that this/these peptides will be useful in the crystallization of the RPA/Rad52 complex. These data are presented in the figures below. An abstract for a poster presentation on this research is included in the appendix: D. Jackson, K. Dhar, M. Wold and G. E. O. Borgstahl "Analysis of the Rad52/RPA Complex: Evidence for Crosstalk Between RPA32, RPA70, Rad52 and ssDNA", Era of Hope Meeting, Orlando, Florida, September, 2002.

RPA70 and RPA32 binding sites on Rad52
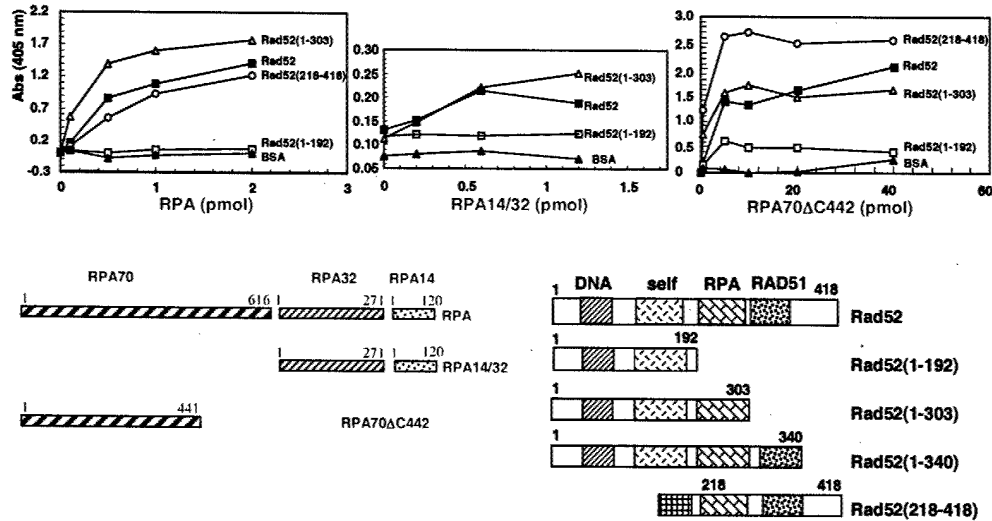
RPA70 and RPA32 both interact with amino acids 218-303 of Rad52.

## Does RPA32 have a separate site on Rad52 or compete with RPA70?
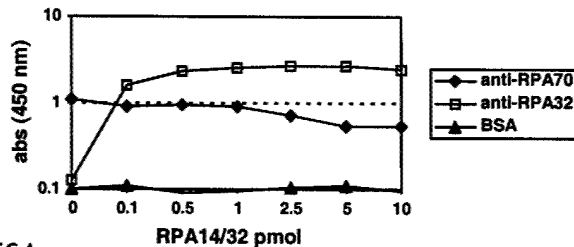
Competitive ELISA
- Coated plate with 10 pmol of Rad52 and washed.
- Knew 5 pmol RPA70ΔC442 saturated the complex with Rad52.
- 5 pmol of RPA70ΔC442 was mixed with a varying amount of RPA14/32 and added to the plate.
- anti-RPA1 detects RPA70ΔC442 and anti-RPA2 detects RPA14/32
- Detection with anti-RPA1 and anti-RPA2 was performed in separate wells.

Binding site determinants for RPA70 and RPA32 are separate on each subunit of Rad52. At high amounts of RPA14/32 there is competition with RPA70.

In the report from last year we reported results on differential scanning calorimetry data on wild-type and mutant human Rad52. Wild-type and mutant hRad52

data showed that the wild-type protein has extreme thermal stability (T_M 115 °C). The N-terminal half is responsible for ring formation and the C-terminal half participates in the higher order self-association of rings. This work was written up and published in Biochemistry last year.

The study of the protein-protein interactions and thermal stability of Rad52 was extended to the homologous Rad52 from *S. cerevisia*. We developed purification protocols for wild-type and mutant scRAD52. By calorimetry, we found that the scRad52 was less stable than human and that the quaternary structure of the N-terminal mutant of scRad52 was less stable than in humans. Figures of these data are presented below. An abstract for a poster presentation on this research at the Era of Hope meeting is included in the appendix: W. Ranatunga, D. Jackson and G. E. O. Borgstahl "Temperature Modulates the Higher-ordered Self-association of Rad52", Era of Hope Meeting, Orlando, Florida, September, 2002.

scRAD52 proteins expressed and purified
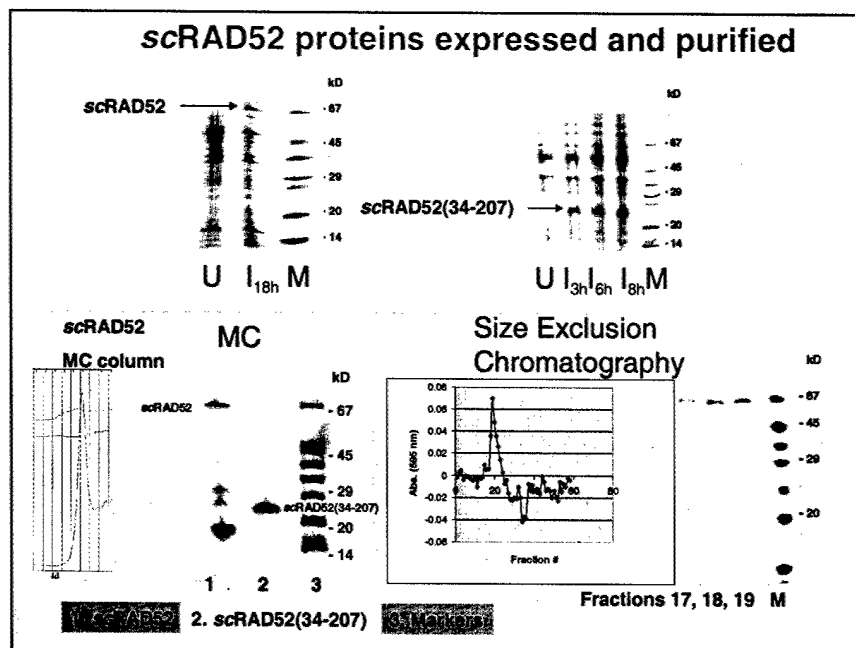
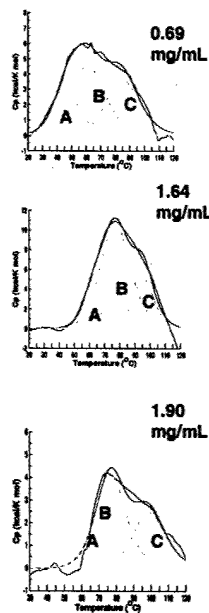## scRAD52 is not stable as scRAD52(34-207)

(DSC profiles)
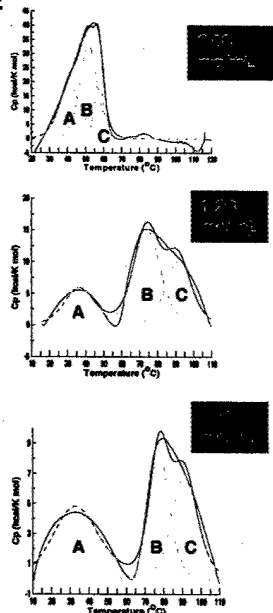
scRAD52   **scRAD52(34-207)**

DSC melting temperatures for hRAD52 and scRAD52 proteins in nano-DSC

Line #	Protein	Comp.	Conc.	T_M (°C)	Conc.	T_M (°C)	Conc.	T_M (°C)	Conc.	T_M (°C)
1	scRAD52	A	0.58	41.4	0.66	34.3	1.3	37.0	2.5	33.7
		B		51.8		48.1		74.1		77.9
		C		57.5		88.2		91.7		91.5
2	scRAD52 (34-207)	A	0.69	47.6	0.76	59.8	1.6	62.5	1.9	60.2
		B		62.0		74.7		77.5		77.1
		C		85.6		84.4		96.0		99.3
3	hRAD52	A	0.50	38.7	0.52	38.5	1.2	36.3	2.5	35.2
		B		80.5		74.2		75.5		78.8
		C		89.9		90.1		90.8		96.1
4	hRAD52 (1-192)	B	0.45	40.4	0.69	41.1	1.2	43.0	2.3	56.0
		C'								78.4
		C		78.1		80.9		85.8		93.9

These results will be published in the remaining year of the grant.

<u>Objective 4:</u> ***Test the feasibility of crystallizing the phosphorylated proteins obtained in objectives 1 and 2 and perform crystallization trials on the proteins obtained in objective 3.***

Several soluble active fragments (SAF) of RAD52 have been obtained for crystallization. Crystallization efforts have been continuously underway this year with no reportable outcomes. Of brighter note, several crystal forms of RPA heterodimer have been grown in four different space groups and excellent diffraction data collected at the synchrotron. A manuscript reporting the use of dynamic light scattering to promote crystallization and to study the self association of RPA14/32 was published in Acta Crystallographica D. A reprint of this manuscript was included in the appendix of last years report. One abstract of a poster presentation by my postdoctoral fellow at the national American Crystallographic Association conference was also included in last years report. The solution of this structure by MAD phasing continued this year and the structure is still in progress.

<u>Significance – first RPA14/32 structure.</u> The crystal structure of human RPA14/32 will reveal for the first time the structure of the intact RPA32 subunit, including the N-terminus, which is hyperphosphorylated during apoptosis and in response to DNA damage, and the C-terminal domain, which interacts with several DNA metabolic proteins, including Rad52. Comparison of this structure with that of the already determined proteolytic core of RPA14/32 (protein data bank entry 1QUQ) will reveal why the core binds ssDNA weakly while the intact protein does not bind ssDNA [2].

A combination of two phasing methods, molecular replacement and multi-wavelength anomalous dispersion (MAD), are being used to solve the phase problem for the first structure of RPA14/32 [7]. As soon as the first native diffraction data on RPA14/32 were collected, extensive attempts to solve the structure by molecular replacement using the coordinates of RPA14(3-116)/RPA32(45-170) from the protein data bank (entry 1QUQ) were made. Solutions were found and in some cases, weak density for the missing domains could be seen. However, phasing was never sufficient to produce clean maps that could be reliably interpreted for the missing domains. All attempts on all crystal forms failed. There are three possible reasons for this. Entry 1QUQ provides only 56% of the structure in the crystals. RPA14(3-116) and RPA32(45-170) are structurally very similar (see Fig. 4 and Fig. 2 in Bochkarev et al. (1999)) and molecular replacement may put 14 where 32 belongs and vice versa. Finally, perhaps the structure of the full-length RPA14/32 differs from the protease resistant core. Ambiguity between the hexagonal space groups and number of molecules in the asymmetric unit has also been a problem.

Unfortunately, the two MAD datasets reported in last years report were insufficient to completely phase the RPA14/32 crystal [5]. This is most likely due to problems in data quality and some personnel problems. A new student has been recruited to work on this project, he has learned the techniques and he has been very successful this year in growing fresh crystals of RPA14/32 for more data collection. This data collection on heavy atom derivatives will be performed in the last year of the grant.

Purification of several RPA and Rad52 constructs were performed. Unfortunately no crystals grew. Neither protein will crystallize by itself. Light scattering data indicates

that the complex of RPA/Rad52 is more condensed and stable than the holoproteins alone. Crystallization screening will continue into the last year of this award. In particular, as a result of our protein-protein results we will pursue crystals of the full length Rad52 in complex with a peptide of RPA, as well as, the full length RPA in complex with a peptide of Rad52.

Key Research Accomplishments

- Determined the location of the binding site for Rad52 on RPA70 and discovered that the formation of Rad52/RPA complex increases the ssDNA affinity of RPA through DNA binding domain D on RPA32.
- Found that the RPA32 and RPA70 sites on Rad52 were separate but competitive.
- Determined that the RPA70 and the RPA32 binding sites lie within residues 218-313 of Rad52.
- Partially solved of the crystallographic phase problem for crystals of full length human RPA14/32.
- Constructs of phosphorylation mutant of heterotrimeric and dimeric human RPA and yeast RFA were screened for crystallization.
- Purified wild-type and mutant scRAD52, tested for aggregation, screened for crystals and calorimetry data was collected.

Reportable Outcomes

Employment

May 2002   Associate Professor with tenure; The University of Toledo, Department of Chemistry, Toledo, OH.

Aug 2002   Associate Professor with tenure; Eppley Cancer Research Institute, Omaha, NE.

Matriculated with Ph.D. in Chemistry:

1. Wasantha Ranatunga, "Expression, purification, biophysical characterization and preliminary crystallization of human and yeast RAD52 proteins", July 24, 2002.

2. Doba Jackson, "Analysis of the human Rad52/RPA complex: characterization of the interacting regions, DNA binding activity, and higher-order complexes", July 31, 2002.

Manuscripts, abstracts, presentation (attached in appendix):

1. Abstract for poster presentation: W. Ranatunga, D. Jackson and G. E. O. Borgstahl "Temperature Modulates the Higher-ordered Self-association of Rad52", Era of Hope Meeting, Orlando, Florida, September, 2002.

2. Abstract for poster presentation: D. Jackson, K. Dhar, M. Wold and G. E. O. Borgstahl "Analysis of the Rad52/RPA Complex: Evidence for Crosstalk Between RPA32, RPA70, Rad52 and ssDNA", Era of Hope Meeting, Orlando, Florida, September, 2002.

3. Reprint of publication: D. Jackson, K. Dhar, J. K. Wahl, M. S. Wold and G. E. O. Borgstahl, G. E. O. "Analysis of the Rad52/RPA Complex: Evidence for Crosstalk Between RPA32, RPA70, Rad52 and ssDNA" *J. Mol. Biol.* **321**, 133-148 (2002).

Research Proposal activity

1. "Structural Studies on Replication Protein A" Borgstahl PI, American Cancer Society Research Scholars Grant for Beginning Investigators, Funded, Total budget $720,000 for 4 years. *This proposal was ranked 1/57 by the Genetic Mechanisms in Cancer Committee and rated as "Outstanding".*

Conclusions

Protein-protein interactions between RPA and RAD52 are important in the first step of the double-strand break repair pathway. RPA is phosphorylated in a cell-cycle dependent manner and by several enzymes *in vitro* including AT kinase. The role of RPA phosphorylation is not well understood, but it does not appear to modulate the interaction of RPA with RAD52. Interestingly, RPA phosphorylation has recently been shown to promote the dissociation of RPA14/32 dimer from the RPA70 subunit. In the final year of this award we will continue to investigate the structural consequences of phosphorylation on RPA structure in the context of the RPA heterotrimer and the dimer. Mutation of Thr and Ser to Asp will be used to mimic phosphorylation. To date, only proteolytically stable core fragments of RPA have been crystallized and their structures solved. During year 1, of this award the full-length RPA14/32 dimer was crystallized in two crystal forms, many sets of X-ray diffraction data were collected and the structure will be solved in the second year of this award. RAD52 was been found to aggregate in solution and electron micrograph studies show that it forms ring structures in solution. These aggregates are polydisperse with 8-10 monomers per ring and multiple rings can associate to form higher molecular weight aggregates. Such aggregation has been problematic for crystallization. Fortunately, we have found several suitable constructs that are soluble and retain single-stranded DNA binding and/or RPA binding activities. During year 2, the crystallization of RPA14/32 was further extended and more data was collected and a manuscript concerning this work was published. Constructs for expression of yeast RFA14/32 and a phosphorylation mimic of human RPA14/32 were created. Dynamic light scattering data and electron micrographs and have delineated the roles of the N- and C-terminal halves of RAD52 in ring formation and super ring aggregation. Differential scanning calorimetry data demonstrated the extreme thermal stability of RAD52 and stimulated new ideas on how to crystallize and purify RAD52. Crystallization trials for all constructs discussed are continuing. Structural determination of these proteins by X-ray crystallography will reveal a wealth of information on how they function in double-strand break repair. In year 3, several manuscripts were prepared and published. Key information on the effect of Rad52 binding to RPA on ssDNA affinity and Rad52 self-association were made. The crystallographic phase problem for human RPA14/32 was partially solved. In year 4, the details of the contact regions of the RPA/Rad52 complex and the effect of the RPA/Rad52 complex on the ssDNA affinity was published. Wild-type and mutant scRad52 was purified and screened for crystals. Interesting calorimetric data for scRad52 was obtained. New crystals of RPA14/32 were obtained for solution of the phase problem. The laboratory moved to the Eppley Cancer Research Institute.

References

1. Bertwistle, D. and A. Ashworth, *Functions of the BRCA1 and BRCA2 genes.* Curr. Opin. Genet. Dev., (1998). **8**, 14-20.
2. Bochkareva, E., L. Frappier, A.M. Edwards and A. Bochkarev, *The RPA32 Subunit of Human Replication Protein A Contains a Single-stranded DNA-binding Domain.* J. Biol. Chem., (1998). **273**, 3932-3936.
3. Bourgeois, D., *New processing tools for weak and/or spatially overlapped macromolecular diffraction patterns.* Acta Cryst., (1999). **D55**, 1733-1741.
4. Dauter, Z., M. Dauter and K.R. Rajashankar, *Novel approach to phasing proteins: derivatization by short cryo-soaking with halides.* Acta Cryst., (2000). **D56**, 232-237.
5. Doublie, S., *Preparation of selenomethionyl proteins for phase determination.* Methods Enzymol., (1997). **276**, 523-530.
6. Gately, D.P., J.C. Hittle, G.K.T. Chan and T.J. Yen, *Characterization of ATM Expression, Localization and Associated DNA-dependent Protein Kinase Activity.* Mol. Biol. Cell, (1998). **9**, 2361-2374.
7. Hendrickson, W.A. and C.M. Ogata, *Phase Determination from Multiwavelength Anomalous Diffraction Measurements.* Methods Enzymol., (1997). **276**, 494-523.
8. Lavin, M., *Role of the ataxis-telangiectasia gene (ATM) in breast cancer.* BMJ, (1998). **317**, 486-487.
9. McRee, D.E., *Practical Protein Crystallography.* 1993, San Diego, CA: Academic Press, Inc.
10. Park, M.S., D.L. Ludwig, E. Stigger and S.H. Lee, *Physical interaction between Human RAD52 and RPA is Required for Homologous Recombination in Mammalian Cells.* J. Biol. Chem., (1996). **271**, 18996-19000.
11. Read, R.J., *Model phases: Probabilities and bias.* Methods Enzymol., (1997). **277**, 110-128.
12. Shinohara, A. and T. Ogawa, *Homologous recombination and the roles of double-strand breaks.* Trends Biochem Sci, (1995). **20**, 387-391.
13. Terwilliger, T.C., *Maximum-likelihood density modification.* Acta Cryst., (2000). **D56**, 965-972.
14. Terwilliger, T.C. and J. Berendzen, *Automated structure solution for MIR and MAD.* Acta Cryst., (1999). **D55**, 849-861.
15. Wold, M.S., *RPA: A Heterotrimeric, Single-Stranded DNA-Binding Protein Required for Eukaryotic DNA Metabolism.* Ann. Rev. Biochem., (1997). **66**, 61-91.

TEMPERATURE MODULATES THE HIGHER-ORDERED SELF-ASSOCIATION OF RAD52

Wasantha Ranatunga, Doba Jackson, and Gloria E. O. Borgstahl

Department of Chemistry, The University of Toledo,
2801 West Bancroft Street, Toledo, OH 43606

wranatunga@hotmail.com

Defects in recombination-based DNA repair lead to human breast cancer and familial degenerative diseases. The RAD52 epistasis gene products, especially the human RAD52 protein plays important role in double-strand break (DSB) repair. hRAD52 has shown to be interacting with many proteins in recombination-based DSBs repair pathway. The focus of this work is to further understanding of the molecular basis of DSBs by solving the three-dimensional structure of hRAD52. The hRAD52 forms ring structure in solution and multiple level of aggregation of rings.

Due to the biological interest of hRAD52 and the apparent biochemical importance of RAD52 self-association in DNA-repair, we studied its multiple levels of self-association and stability using biophysical methods such as dynamic light scattering (DLS) and differential scanning calorimetry (DSC). The stability of wild-type RAD52 was studied by DSC. To investigate the basis for the extreme stability of RAD52 that was discovered, two mutants were also studied, RAD52 (1-192) and RAD52 (218-418). The effects of temperature and protein concentration on the hydrodynamic radius (RH) of RAD52 were studied by DLS.

We found that the aggregation is due to two levels of self-association of hRAD52, ring formation and association of rings with rings. DSC profiles and DLS data indicated that hRAD52 protein is extremely stable and multiple levels of self-association of hRAD52 can be disrupted by heating up to 50 °C.

A hypothetical model of the effects of protein aggregation state on thermal stability was developed. Based on these findings, a novel approach for purification of hRAD52 and for crystallization was established. This research will contribute a detailed understanding of the molecular mechanisms of breast cancer.

ANALYSIS OF THE RAD52/RPA COMPLEX: EVIDENCE FOR CROSSTALK BETWEEN RPA32, RPA70, RAD52, AND SSDNA

Doba Jackson, Kajari Dahr, Marc Wold, and Gloria Borgstahl

University of Toledo, Toledo, OH

djackso2@uoft02.utoledo.edu

The eukaryotic single-stranded DNA-binding protein, replication protein A (RPA), is essential for DNA replication, and plays important roles in DNA repair and DNA recombination. Rad52 and RPA, along with other members of the Rad52 epistasis group of genes, repair double-stranded DNA breaks (DSBs). Two repair pathways involve RPA and Rad52, homologous recombination and single-strand annealing. Two binding sites for Rad52 have been identified on RPA. They include the previously identified C-terminal domain (CTD) of RPA32 (residues 224 to 271) and the newly identified domain containing residues 169 to 326 of RPA70. A region on Rad52, that includes residues 218 to 303, binds RPA70 as well as RPA32. The N-terminal region of RPA32 does not appear to play a role in the formation of the RPA:Rad52 complex. It appears that the RPA32CTD can substitute for RPA70 in binding Rad52. Sequence homology between RPA32 and RPA70 was used to identify a putative Rad52 binding site on RPA70 that is located near DNA binding domains A and B. Rad52 binding to RPA increases ssDNA affinity significantly. Mutations in DBD-D on RPA32 show that this domain is primarily responsible for the ssDNA binding enhancement. RPA binding to Rad52 inhibits the higher-order self-association of Rad52 rings. Implications for these results for the "hand-off" mechanism between protein-protein partners, including Rad51, in homologous recombination and single-strand annealing are discussed..

1

JMB

Analysis of the Human Replication Protein A:Rad52 Complex: Evidence for Crosstalk Between RPA32, RPA70, Rad52 and DNA

Doba Jackson[1], Kajari Dhar[2], James K. Wahl[3], Marc S. Wold[2] and Gloria E. O. Borgstahl[1]*

[1]*Department of Chemistry University of Toledo 2801 West Bancroft Street Toledo, OH 43606-3390, USA*

[2]*Department of Biochemistry University of Iowa College of Medicine, 51 Newton Road Iowa City, IA 52242-1109 USA*

[3]*Department of Biology University of Toledo, Toledo OH 43606-3390, USA*

The eukaryotic single-stranded DNA-binding protein, replication protein A (RPA), is essential for DNA replication, and plays important roles in DNA repair and DNA recombination. Rad52 and RPA, along with other members of the Rad52 epistasis group of genes, repair double-stranded DNA breaks (DSBs). Two repair pathways involve RPA and Rad52, homologous recombination and single-strand annealing. Two binding sites for Rad52 have been identified on RPA. They include the previously identified C-terminal domain (CTD) of RPA32 (residues 224–271) and the newly identified domain containing residues 169–326 of RPA70. A region on Rad52, which includes residues 218–303, binds RPA70 as well as RPA32. The N-terminal region of RPA32 does not appear to play a role in the formation of the RPA:Rad52 complex. It appears that the RPA32CTD can substitute for RPA70 in binding Rad52. Sequence homology between RPA32 and RPA70 was used to identify a putative Rad52-binding site on RPA70 that is located near DNA-binding domains A and B. Rad52 binding to RPA increases ssDNA affinity significantly. Mutations in DBD-D on RPA32 show that this domain is primarily responsible for the ssDNA binding enhancement. RPA binding to Rad52 inhibits the higher-order self-association of Rad52 rings. Implications for these results for the "hand-off" mechanism between protein–protein partners, including Rad51, in homologous recombination and single-strand annealing are discussed.

© 2002 Elsevier Science Ltd. All rights reserved

Keywords: human Rad52; replication protein A; double-strand break repair; protein–protein interaction; single-stranded DNA binding

*Corresponding author

Introduction

The repair of double-strand breaks (DSBs) in chromosomal DNA is of critical importance for the maintenance of genomic integrity. In *Saccharomyces cerevisiae*, genes of the RAD52 epistasis group were identified initially by the sensitivity of mutants to ionizing radiation.[1] These genes have been implicated in an array of recombination events, including mitotic and meiotic recombination as well as DSB repair. The importance of specific protein–protein interactions in the catalysis of homologous recombination is suggested by studies that demonstrate specific contacts and functional interactions between scRad52, scRPA and scRad51.[2–6] Studies of the equivalent human proteins have identified similar interactions.[7–9]

Rad52 protein plays a critical role in mitotic and meiotic recombination as well as DSB repair.[1] On the basis of a series of protein–protein interaction assays and DNA-binding studies, a domain map of human Rad52 was proposed (shown in Figure 1).[10]

Abbreviations used: C_p, polydispersity; CTD, C-terminal domain; DBD, DNA-binding domain; DLS, dynamic light-scattering; DSB, double-strand break; EM, electron microscopy; GMSA, gel mobility-shift assay; mAb, mouse monoclonal antibody; OB-fold, oligonucleotide/oligosaccharide binding; Rad52, human Rad52 protein; R_H, hydrodynamic radius; RPA, human replication protein A; RPA14, 14 kDa subunit of RPA; RPA32, 32 kDa subunit of RPA; RPA70, 70 kDa subunit of RPA; scRad52, *Saccharomyces cerevisiae* Rad52; scRPA, *Saccharomyces cerevisiae* RPA; SLS, static light-scattering; SOS, sum of squares; SPR, surface plasmon resonance; ssDNA, single-stranded DNA.

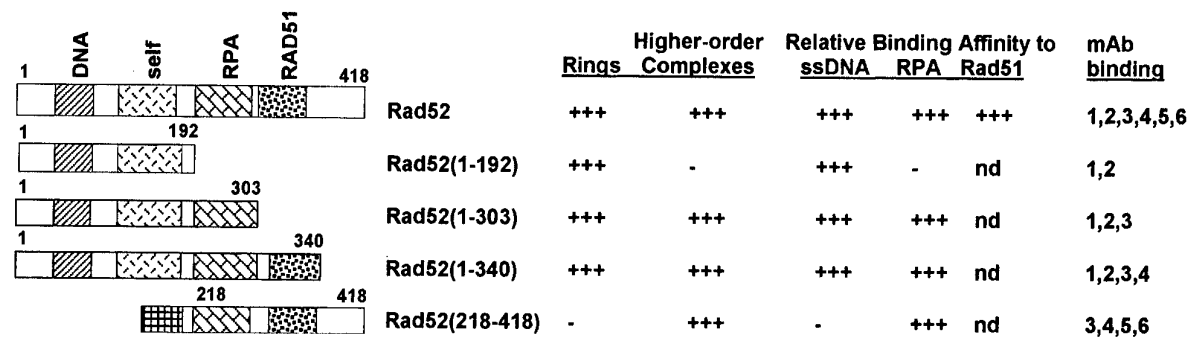E-mail address of the corresponding author: gborgst@uoft02.utoledo.edu

		Rings	Higher-order Complexes	Relative Binding Affinity to			mAb binding
				ssDNA	RPA	Rad51	
	Rad52	+++	+++	+++	+++	+++	1,2,3,4,5,6
	Rad52(1-192)	+++	-	+++	-	nd	1,2
	Rad52(1-303)	+++	+++	+++	+++	nd	1,2,3
	Rad52(1-340)	+++	+++	+++	+++	nd	1,2,3,4
	Rad52(218-418)	-	+++	-	+++	nd	3,4,5,6

Figure 1. A diagram of the Rad52 domain structure, Rad52 mutants used and characterization of monoclonal antibodies developed against Rad52. Rad52 interaction domains with the residue numbers in parentheses were defined as follows: DNA-binding domain (residues 25–65), Rad52 heptameric ring binding (125–185), RPA32 binding (220–280), Rad51-binding domain (290–340).[10,14,53] Wild-type and mutant Rad52 are shown to the left with domains indicated and beginning and ending residue numbers included. Wild-type Rad52, Rad52(1–192), Rad52(1–303) and Rad52(1–340) pET28 expression plasmids were a gift from Dr Min Park and have six histidine residues fused to the C-terminus. For improved solubility, the Rad52(218–418) mutant has thioredoxin fused to the N terminus. This thioredoxin was modified with six histidine residues fused to its N terminus to improve purification. Characterization of each construct for ring structure, higher-order complexes, relative binding affinity for ssDNA, RPA and Rad51, as well as monoclonal antibody binding are summarized on the right.[14]

Rad52 has a homologous pairing activity thought to be important in Rad51-independent DSB repair, and this activity was localized to residues 1–237.[11] Electron microscopy (EM) studies of *S. cerevisiae* and human Rad52 have revealed formation of ring-shaped structures (9–13 nm in diameter), as well as higher-order aggregates.[4,9,12] The Rad52 rings appear to be composed of seven subunits.[13] EM studies showed that Rad52 binds to DNA ends as an aggregated complex that ranges in size from approximately 15–60 nm in diameter.[12] This binding has been found to promote end-to-end association between DNA molecules and to stimulate the ligation of both cohesive and blunt DNA ends. Recently, the studies with wild-type and two deletion mutants of Rad52 have demonstrated that the self-association domain in the N-terminal half of Rad52 is responsible for ring formation and that elements in the C-terminal half of the molecule participate in the formation of higher-order complexes of rings.[11,14] Such higher-ordered complexes of Rad52 rings have been shown by EM to mediate single-strand annealing.[15]

RPA is the single-stranded DNA (ssDNA) binding protein that has been found in all eukaryotes examined.[16,17] It is composed of three subunits that have been named for their molecular mass as RPA70, RPA32 and RPA14 (Figure 2). All three subunits of RPA are required for function. All RPA homologs bind ssDNA with high affinity and participate in specific protein–protein interactions. RPA binds tightly to ssDNA with apparent association constants of 10^9–10^{10} M^{-1} and prefers polypyrimidine sequences to polypurine sequences.[18-20] The major binding mode for RPA has an occluded binding site of 30 nucleotides per RPA heterotrimer.[21] The major ssDNA binding site is located in the middle of RPA70 and is composed of two structurally conserved oligonucleotide/oligosaccharide binding (OB) domains[19,22] called

DBD-A (including residues 181–290) and DBD-B (residues 300–422). To date, four additional OB-folds have been identified in RPA. The N terminus (residues 1–110; called RPA70NTD), the C terminus of RPA70 (residues 432–616; called DBD-C), the central core of RPA32 and the core of RPA14 are all composed of OB-folds.[23-26] RPA is known to undergo a significant conformational change upon binding DNA.[19,27] This conformational shift has been suggested to alter the structure of RPA in a way that facilitates phosphorylation and interactions with other proteins.[27]

RPA is phosphorylated during the S phase of the cell-cycle, in response to DNA damage and during apoptosis.[27-29] The primary phosphorylation sites are located in the N-terminal 33 amino acid residues of RPA32. This DNA damage-induced phosphorylation is coincident with cell-cycle arrest and loss of the ability of cell extracts to support DNA replication[30,31] and in some studies leads to disassembly of the RPA heterotrimer complex.[32] The RPA complex appears to contain all three subunits at sites of ongoing DNA replication.[33,34] These observations suggest that phosphorylation of RPA serves as a mechanism for modulating RPA activity, quaternary structure and its interactions with other proteins. RPA mutants, designed to mimic biological phosphorylation by replacing Ser or Thr with Asp, have been shown to modify the activity of RPA (Braun & M.S.W., unpublished results).

RPA has specific interactions with many proteins; such as replication proteins T antigen, DNA polymerase, and DNA primase; the tumor suppressor p53; transcription factors Gal4 and VP16; and DNA repair factors, XPA, ERCC-1/XPF nuclease, XPG, uracil DNA glycosylase, Rad52 and Rad51.[10,16,17,35-38] Interactions between Rad51, Rad52, and RPA stimulate homologous recombination-based DSB repair.[5,7,8,39] An interaction region of RPA with Rad51 was located between residues
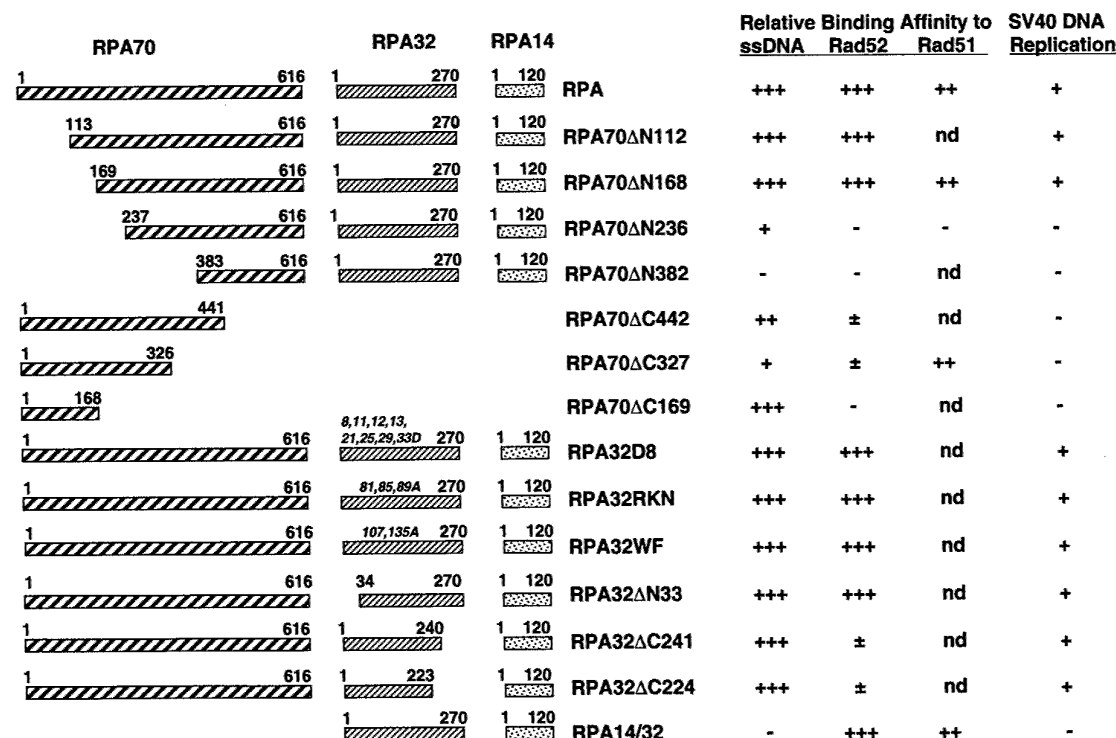
	Relative Binding Affinity to			SV40 DNA
	ssDNA	Rad52	Rad51	Replication
RPA	+++	+++	++	+
RPA70ΔN112	+++	+++	nd	+
RPA70ΔN168	+++	+++	++	+
RPA70ΔN236	+	-	-	-
RPA70ΔN382	-	-	nd	-
RPA70ΔC442	++	±	nd	-
RPA70ΔC327	+	±	++	-
RPA70ΔC169	+++	-	nd	-
RPA32D8	+++	+++	nd	+
RPA32RKN	+++	+++	nd	+
RPA32WF	+++	+++	nd	+
RPA32ΔN33	+++	+++	nd	+
RPA32ΔC241	+++	±	nd	+
RPA32ΔC224	+++	±	nd	+
RPA14/32	-	+++	++	-

Figure 2. Schematic of the RPA and RPA mutants used. The left portion shows diagrams of all RPA mutants used in this study. Beginning and ending amino acid residues of each mutant are indicated. The strength of the protein–protein interactions between RPA and Rad52 are indicated as follows (the data are summarized in Figure 1): (1) Strong complex forming (+++); (2) weak complex forming (±); (3) no complex forming (−). ELISA was used to determine protein–protein interactions with RPA mutants and Rad52 in this study. Only an interaction twofold above that of BSA was considered as a weak binding interaction, and the no complex forming proteins did not show a signal twofold above that of BSA even at higher concentrations (data not shown). Protein interactions with Rad51 by RPA and Rad52 mutants were determined in previous work.[37] ssDNA binding and SV40 DNA replication activities of the RPA mutants were determined in previous studies.[20,35,42] The nomenclature used for each RPA mutant is summarized below. Deletions from the N or C terminus are indicated by a RPA, (subunit of residues deleted—70,32), followed by Δ, then the terminus where the deletions occurred (N or C) and the amino acid residue number where the deletion started (for C-terminal deletions) or the last amino acid residue deleted (for N-terminal deletions). RPA32D8 has the following mutations S8D, S11D, S12D, S13D, T21D, S25D, S29D, and S33D, to mimic hyperphosphorylated RPA (Braun & M.S.W. unpublished results). RPA32RKN has the following mutations R81A, K85A, N89A in the putative ssDNA binding site of RPA32. RPA32WF has the following mutations W107A and F135A in the putative ssDNA binding site of RPA32.

168 and 236 of RPA70.[37] RPA14/32 also co-immunoprecipitated with Rad51 but the interaction with RPA32 was not explored further.[37] The interaction sites on RPA for Rad52 have not been mapped carefully. Human Rad52 was shown to interact strongly with RPA32 and weakly with RPA70.[10] Park and co-workers cited unpublished results that the acidic C terminus of RPA32 (including the last 33 amino acid residues) interacted with the basic patch of residues they had identified on Rad52.[10] Recently, a C-terminal fragment of RPA32 composed of residues 172–270 was studied by NMR, alone and in complex with peptides of UNG2, XPA and Rad52 (including residues 257–274).[40] Yet, the co-precipitation of RPA70 as well as RPA32 with Rad52 by Park indicated that the C terminus of RPA32 is only part of the Rad52 interaction surface. Two-hybrid and co-precipitation analysis of yeast proteins gave additional

evidence of the involvement of scRPA70 as well as scRPA32 in the interaction with scRad52.[38]

Since the interaction of Rad52 with RPA is important in DSB repair and the literature provides an incomplete description of the RPA surface that interacts with Rad52, the regions of RPA involved in binding Rad52 have been explored in detail. The protein–protein interactions of several mutants of RPA with Rad52 have been studied to define the role of the N or C terminus of RPA32, RPA phosphorylation and RPA70 in the RPA:Rad52 interaction. Our results reveal that the interaction of Rad52 with RPA involves two binding sites, one on RPA70 and one on RPA32. These results motivated a homology search that identified a putative Rad52-binding site near the major ssDNA-binding site of RPA70. A mixture of RPA:Rad52 has higher affinity for ssDNA than either RPA or Rad52 alone, and this increase
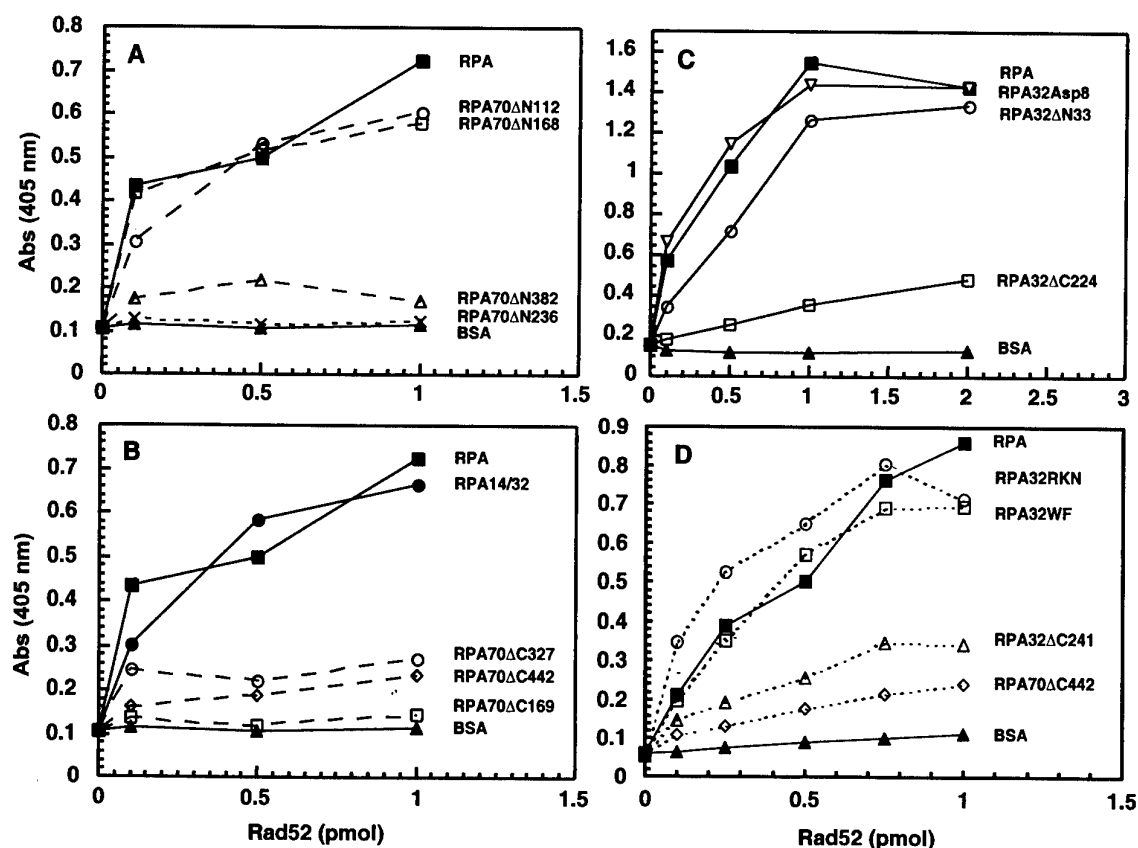
Figure 3. Deconvolution of the domains on RPA that bind Rad52. In the ELISA assay, wild-type or mutant RPA was immobilized on a microtiter plate. Increasing amounts of wild-type Rad52 were added to plates and washed. The bound Rad52 was detected with a specific monoclonal Rad52 antibody (mAb6, see Figure 1) followed by a peroxidase-coupled anti-mouse IgG antibody. Interactions were monitored by measuring ABTS absorbance at 405 nm after the addition of substrate and plotted against the amount of Rad52. (a) RPA and heterotrimeric mutants of RPA70, (b) RPA, RPA14/32 and RPA70 mutants, (c) RPA and heterotrimeric mutants of RPA32, and (d) RPA, heterotrimeric point mutants, RPA70 mutant and heterotrimeric mutant of RPA32. Multiple assays were performed and representative data are shown.

appears to be through increased affinity of RPA32 for ssDNA. Finally, by studying the size of the RPA:Rad52 complex in comparison to Rad52 and RPA alone, it was found that the interaction of RPA with Rad52 disrupts the higher-order aggregation of Rad52 rings and promotes single Rad52 rings in solution. Taken together with the similarity between Rad52 and Rad51-binding sites on RPA, these studies provide a molecular basis for Rad51 and Rad52 competition for binding to RPA. This competition between the protein–protein interaction surfaces of Rad52, Rad51 and RPA is likely to be critical for efficient DSB repair. The higher affinity of the RPA:Rad52 complex for ssDNA has implications for the mechanism of single-strand annealing.

Results

Identification of the regions of RPA important for binding Rad52

The association of Rad52 to RPA was studied using an ELISA method with purified Rad52,

wild-type and several mutant forms of RPA (Figure 2). For the ELISA, RPA was immobilized on a microtitre plate, excess sites were blocked with 5% milk and increasing concentrations of hRad52 were added, incubated and washed. Any Rad52 in complex with RPA or RPA mutants was then detected with a monoclonal antibody (mAb6, see Figure 1) that recognizes an epitope between residues 341 and 418 on the C terminus of Rad52. RPA heterotrimer deletion mutants in the N-terminal region of RPA70 are shown in Figure 3(a). In Figure 3(b), RPA heterotrimer was compared with the heterodimer and peptides of RPA70. In Figure 3(c) and (d), data on RPA heterotrimer mutants with deletions or mutations in RPA32 are shown in comparison to RPA heterotrimer and residues 1–441 of RPA70. The RPA mutants used here were used previously to map the regions of RPA binding to Rad51, XPA, DNA polymerase and T-antigen.[35,37,41,42]

Five primary conclusions were made on the basis of the ELISA data. First, Rad52 binding was reduced significantly when residues 224–271
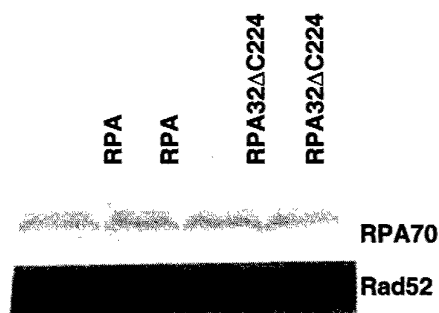
Figure 4. Immunoprecipitation of RPA:Rad52 and RPA32ΔC224:Rad52 complex. Reactions (in duplicate) in lanes 1 and 2 contained wild-type RPA, and lanes 3 and 4 contained RPA32ΔC224 as indicated. Only the data for antibody mAb3 are shown. All other antibodies gave similar results.

(Figure 3(c)) or residues 241–271 (Figure 3(d)) in the C-terminal domain (CTD) of RPA32 were deleted. This indicates a major role for the acidic C terminus of RPA32 in binding Rad52 and is consistent with previous results and predictions.[10,40] Second, when the N terminus of RPA32 is either deleted or mutated with changes from serine or threonine to aspartic acid (RPA32ΔN33, RPA32Asp8, Figure 2), there is no effect on Rad52 binding. Therefore, the N terminus of RPA32, in either its neutral or acidic/hyperphosphorylated form, is probably not involved in the RPA:Rad52 interaction (Figure 3(c)). Third, Rad52 binding was destroyed when residues 169–382 were deleted from RPA70 in the trimer (Figure 3(a)). It is interesting that deletion of this region of RPA70 disrupts Rad52 binding even though intact RPA32 is present. Fourth, all RPA70 peptides (which lack RPA14/32) bind Rad52 weakly, except RPA70ΔC169, which does not bind at all (Figure 3(b)). This result is consistent with those observed with the RPA heterotrimer mutants with N-terminal deletions in RPA70: no significant change in binding was observed when residues 1–112 or 1–168 were deleted (Figure 3(a)). Fifth, RPA14/32 binds Rad52 as tightly as the heterotrimer (Figure 3(b)), even though RPA70 is not present. In summary, these results show that the RPA:Rad52 complex is negatively affected when either residues 224–271 of RPA32 or residues 169–326 of RPA70 are missing from heterotrimeric RPA.

In immunoprecipitation reactions (Figure 4), a strong and significant interaction was seen between RPA and wild-type Rad52 and between RPA32ΔC224 and wild-type Rad52. All six anti-Rad52 antibodies pull down both the RPA:Rad52 complex and RPA32ΔC224 complex. The level of RPA32ΔC224 in a complex with Rad52 relative to wild-type RPA were similar. There appear to be some differences in the binding of Rad52 to RPA32ΔC224 in the two assays (Figures 3(c) and 4). However, it is difficult to compare the data obtained in the ELISA and immunoprecipitation reactions qualitatively, because RPA was in excess
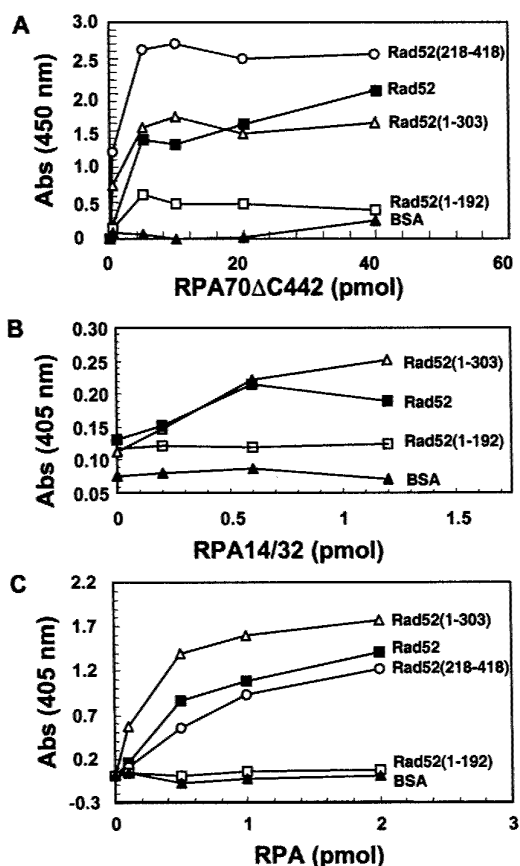

Figure 5. The binding of RPA70ΔC442, RPA14/32 and wild-type RPA to Rad52. In the ELISA assay, wild-type or mutant Rad52 was immobilized on a microtiter plate. Increasing amounts of RPA were added to plates and washed. The bound Rad52 was detected with monoclonal antibodies to RPA70 or RPA32 (Calbiochem) followed by a peroxidase-coupled anti-mouse IgG antibody. Interactions were monitored by measuring TMP substrate absorbance at 450 nm or ABTS substrate at 405 nm and plotted against the amount of RPA.

in the former while Rad52 was in excess in the latter. We conclude that these studies demonstrate a strong interaction between RPA and Rad52 in solution when the RPA32CTD has been deleted, confirming a role for RPA70 in binding Rad52.

The region of Rad52 important for binding RPA32 and RPA70

The interaction site on Rad52 for RPA70 and RPA32 was studied using a similar ELISA protocol. Wild-type or mutant Rad52 was immobilized to a microtitre plate, excess sites were blocked with 5% milk and increasing concentrations of RPA70ΔC442 was added, incubated and washed. Any RPA in complex with Rad52 or Rad52 mutants was then detected with a monoclonal antibody against RPA70 (Calbiochem). The data show that the primary interaction sites for both RPA70 and RPA32 are in the region including Rad52 residues

Table 1. DNA binding activity of forms of RPA, Rad52 and RPA:Rad52 complexes

| GMSA data | | K_A ($\times 10^9$ M^{-1})[a] | | |
RPA forms (ratio)[b]	None	Rad52	Rad52(218–418)
1. None		0.74 (0.24, V)	ND
2. RPA (1:1)	1.4 (0.2, S)	0.75 (0.15, F)	1.3 (0.5, V)
3. RPA (1:7)	1.4 (0.2, S)	7.5 (2.6, S)	25 (6.1, S)
4. RPA14/32 (1:1)	ND	ND	ND

| SPR data[c] | | K_A ($\times 10^8$ M^{-1})[a] | | |
RPA forms (ratio)[b]	None	Rad52	Rad52(218–418)
5. None			ND
6. RPA (1:7)	3.9 (0.5, S)		12 (1.7, S)
7. RPA32RKN (1:7)	2.5 (1.3, S)		1.9 (0.5, S)
8. RPA32WF (1:7)	2.2 (0.6, S)		2.4 (0.8, S)
9. RPA32ΔC224 (1:7)	1.3 (0.1, V)		3.5 (0.2, S)
10. RPA32ΔC241 (1:7)	3.1 (1.6, S)		2.4 (0.7, S)

[a] The error is indicated in parentheses and was estimated from the standard deviation of actual values (indicated by an S), from the variation if only two trials were done (V) or from the fitting error if the experiment was done only once (F); ND, no binding was detected.

[b] RPA:Rad52 complexes were mixed using the ratios indicated where the RPA component is on either the heterotrimer or heterodimer basis and the Rad52 component is on a monomer basis.

[c] Assay done in 1 M KCl.

193–303 (Figure 5). The Rad52(218–418), and Rad52(1–303) showed slightly higher binding activity than wild-type Rad52, perhaps due to increased exposure to the RPA-binding domain.

Effect of Rad52 binding on RPA ssDNA binding

The RPA70 binding site (residues 169–326) for Rad52 identified by protein–protein interaction studies includes all of ssDNA binding site DBD-A and a portion of DBD-B. Therefore, the ability of Rad52 to modulate the affinity of RPA for dT$_{30}$ ssDNA was studied (Table 1 and Figure 6). Using the gel mobility-shift assay (GMSA) under physiological salt concentrations, wild-type RPA had a K_A of 1.4×10^9 M^{-1}, wild-type Rad52 had a K_A of 0.74×10^9 M^{-1}, and no binding was detectable for the Rad52(218–418) mutant (Table 1, rows 1–3; see also Figure 6(a)). Surprisingly, the affinity of the RPA:Rad52 complexes for ssDNA was fivefold to 18-fold higher than RPA or Rad52 alone (Table 1, row 3). The stimulatory effect of the Rad52(218–418) mutant is particularly significant, since this mutant retains the full RPA binding surface but has no detectable affinity for DNA (Table 1, row 3; see also Figure 6(a)).

The effect of the molar ratio of Rad52 monomer to RPA heterotrimer on ssDNA binding affinity of the RPA:Rad52 complexes was studied using GMSA (Table 1 and Figure 6(b)). For wild-type proteins, the 1 to 7 ratio gave maximal binding and the 1 to 14 ratio gave similar binding (Figure 6(b)). Wild-type Rad52 was assumed to be in a heptameric ring. For the RPA:Rad52(218–418) complex, the stoichiometry of binding for the protein–protein complex was not known, so a series of ratios were tested for ssDNA affinity. DNA affinity increased as the ratio increased and was maximal at the 1 to 7 ratio (Figure 6(b)). With

both Rad52 and Rad52(218–418), no stimulation was observed at a 1:1 molar ratio (Table 1, line 2). This suggests that this ratio is too low for a stimulatory interaction or complex to form. Fivefold to 18-fold stimulation was observed at a 1:7 molar ratio (Table 1, row 3). This stimulation was probably not caused by non-specific protein effects, because all reactions contained 50 μg/ml of bovine serum albumin (BSA). These data indicate that the interaction of Rad52 with RPA increases the affinity of RPA for ssDNA significantly, in a Rad52 concentration-dependent manner.

In the GMSA, the affinities of the RPA:Rad52 and RPA:Rad52(218–418) complexes were all high enough to be near or at stoichiometric binding conditions (the apparent K_A determined was close to the concentration of DNA used, 13×10^{-9}M). Under stoichiometric binding conditions, the apparent affinity constant represents a minimum affinity of the complex. Therefore, the stimulatory effect of Rad52 was studied using surface plasmon resonance (SPR) under high-salt conditions in order to obtain equilibrium binding conditions (Table 1, rows 5–10). Raising the salt concentration to 1 M lowered the affinity of RPA for ssDNA by 3.6-fold ($K_A = 3.9 \times 10^8$ M^{-1}). Even under high-salt conditions, the binding of Rad52(218–418) was stimulatory and raised the affinity of RPA threefold to 12×10^8 M^{-1} (Table 1, row 6).

The effect of salt on the RPA:Rad52 complex was then explored through a modified ELISA assay (Figure 7). It was found that salt concentrations higher than 250 mM KCl reduced the wild-type RPA:Rad52 complex by more than 50% under the conditions of the ELISA. At 1 M salt, ~5% of the complex remained (Figure 7(a)). This is not surprising, since the interaction is thought to be mediated partly by electrostatics through an acidic patch on RPA32CTD and a basic patch on Rad52.[10] The
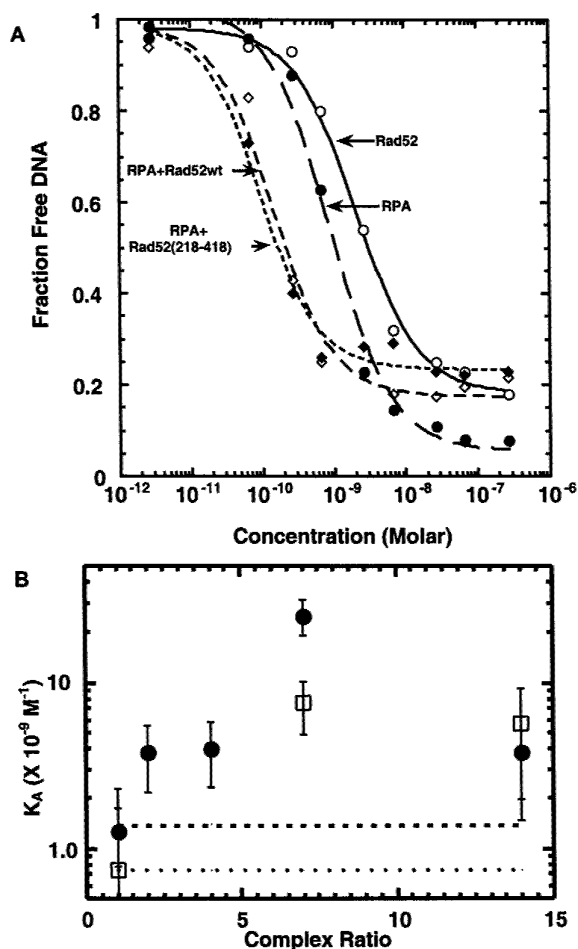
Figure 6. ssDNA binding data for RPA, Rad52 and RPA:Rad52 complexes. (a) Representative ssDNA binding isotherms obtained from GMSA as described in Materials and Methods for RPA (filled circles, long-dash broken line; fitted binding constant $K_a = 1.1 \times 10^9\,\text{M}^{-1}$), Rad52 (open circles, continuous line; $K_a = 0.75 \times 10^9\,\text{M}^{-1}$), RPA:Rad52 (1:7 ratio) complex (open diamonds, short-dash broken line; $K_a = 7.9 \times 10^9\,\text{M}^{-1}$) and RPA:Rad52(218–418) (1:7 ratio) complex (filled diamonds, dotted line; $K_a = 1.3 \times 10^{10}\,\text{M}^{-1}$) Lines are the best fit curves obtained by non-linear least-squares fitting. (b) Binding affinity for ssDNA for RPA, Rad52 and RPA:Rad52 complexes. The measured association constants were measured by GMSA and plotted against the molar ratio of Rad52 monomer to RPA heterotrimer. The broken line indicates the affinity of wild-type RPA heterotrimer and the dotted line indicates the affinity of wild-type Rad52. The affinity of RPA:Rad52 complexes at various ratios of Rad52 to RPA are plotted with open squares for wild-type Rad52, and filled circles for Rad52(218–418). The plotted K_A ($\times 10^9\,\text{M}^{-1}$) values were 0.74 (0.24, V), 0.75 (0.15, F), 7.5 (2.6, S), and 5.6 (3.7, F) for wild-type Rad52 at ratios of 0:1, 1:1, 1:7 and 1:14 to RPA, respectively. For Rad52(218–418) the values were 1.3 (0.5, V), 3.8 (1.6, F), 4.1 (1.7, F), 25 (6.1, S), and 3.9 (2.4, F) at ratios of 1:1, 1:2, 1:4, 1:7 and 1:14 to RPA, respectively.

RPA:Rad52(218–418) complex was studied by SPR and it was slightly more resistant to salt than wild-type, needing more than 400 mM salt to reduce the complex by 50% (Figure 7(c)). At 1 M salt, ~15% of the RPA:Rad52(218–418) complex remained. Results for RPA14/32:Rad52 were similar (Figure 7(b)). The RPA70ΔC442:Rad52(218–418) complex also showed sensitivity to salt and required more than 300 mM salt to reduce the complex by half, and retained 30% of the complex at 1 M salt (Figure 7(d)). This indicates that the majority of the RPA70 interaction is mediated by electrostatic interactions but to a slightly lesser extent than RPA14/32 or the wild-type hetero-trimer. It was concluded that even though the salt conditions of the SPR assay appear to be diminishing the protein–protein interaction between RPA and Rad52, the stimulation of RPA's affinity for ssDNA was still seen (Table 1).

In order to help deconvolute the contributions of RPA70 and RPA32 to the stimulation of ssDNA binding by Rad52(218–418), five mutant forms of RPA were studied (RPA32RKN, RPA32WF, RPA32ΔC224, RPA32ΔC241, and RPA14/32; Figure 2). For the RPA32RKN mutant, conserved polar residues, homologous to those that interact with ssDNA in RPA70,[22] were replaced with alanine. The RPA32WF mutant has two conserved aromatic residues mutated to alanine. Disruption of the corresponding aromatic residues in scRPA has been found to disrupt interactions with DNA of the mutated domain.[23] When binding to a 30 residue oligonucleotide was examined, these mutants have the same affinity as wild-type for ssDNA (Figure 2). This is consistent with previous studies showing that the central domain of RPA70 is primarily responsible for binding to short oligonucleotides.[19] The RPA32RKN and RPA32WF forms of RPA also showed the same affinity for Rad52 as wild-type RPA (Figure 3(d)) but were not stimulated to bind ssDNA by Rad52(218–418) (Table 1, rows 7 and 8). Mutants with the CTD of RPA32 deleted, RPA32ΔC224 and RPA32ΔC241, have diminished binding for Rad52 (Figure 3(d)) and were not stimulated by Rad52(218–418) (Table 1, rows 9 and 10). No binding to ssDNA was detected for the RPA14/32 heterodimer alone or for the RPA14/32:Rad52 complex (Table 1, row 4), indicating that the presence of RPA70 in the RPA complex is required for stimulation. These results show that the increase in DNA affinity of the RPA:Rad52 complex is mediated through DNA binding by RPA32. They suggest that Rad52 binding to both RPA32 and RPA70 is required for stimulation.

RPA binding to Rad52 displaces higher-level self-association of Rad52

Human Rad52 forms large aggregates in solution. Two regions of Rad52 are responsible for aggregate formation (Figure 1). The self-association domain in the N-terminal half of Rad52 is
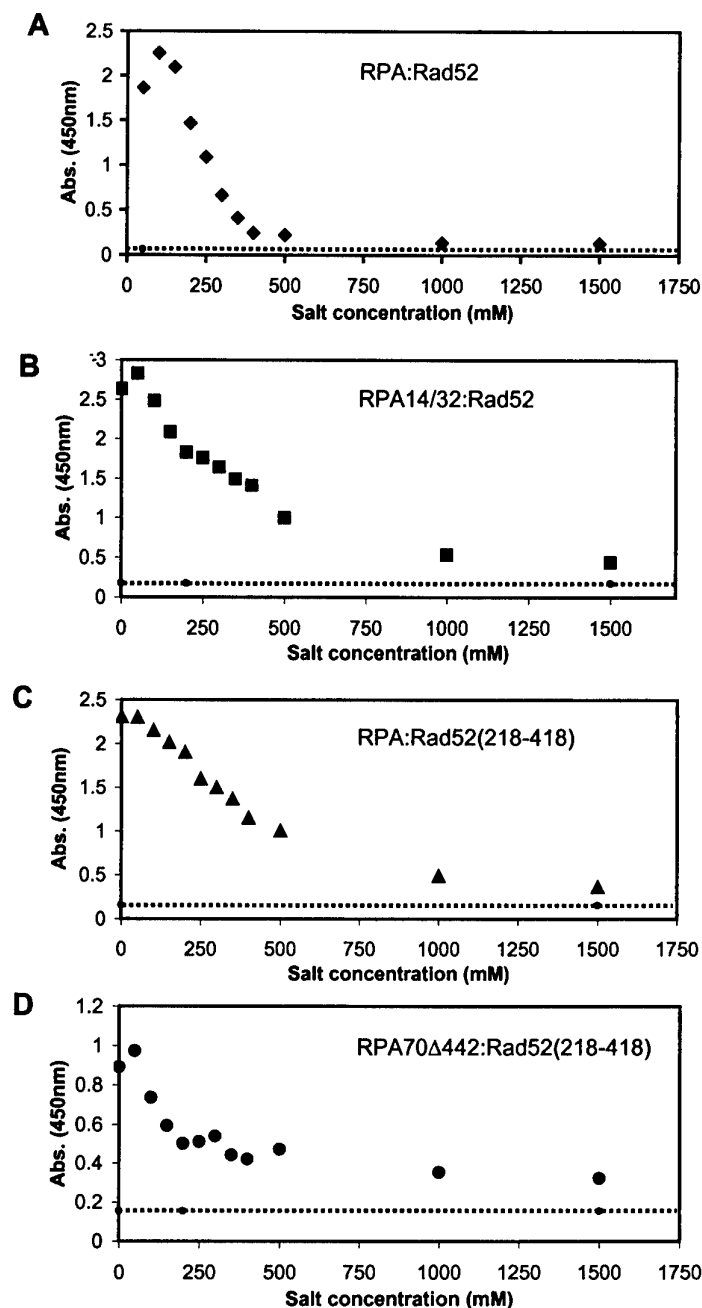
Figure 7. The effect of ionic strength on the RPA:Rad52 complex. A modified ELISA assay using the OPD substrate was used to study the effect of increasing ionic strength on the (a) wild-type RPA:Rad52 complex, (b) RPA14/32:Rad52 complex, (c) RPA:Rad52(218–418) complex, and (d) RPA70Δ442:Rad52(218–418). The dotted line indicates the baseline as determined with BSA. Antibody to RPA70 was used (Calbiochem) to detect wild-type RPA and RPA70ΔC442, and antibody to RPA32 was used to detect RPA14/32.

responsible for heptameric ring-formation and elements in the C-terminal half of the protein participate in the formation of higher-order complexes of rings.[14] The Rad52(218–418) mutant contains the C-terminal elements for the higher-order self-association and does not form rings. Rad52(218–418) contains the binding surface for RPA (Figure 1). The average molecular mass (M) of the proteins and complexes in solution were measured by static light-scattering (SLS) and the ability of Rad52(218–418) to self-associate into higher-ordered complexes in the presence of RPA14/32 and RPA heterotrimer was tested (Table 2 and Figure 8).

Individual proteins were characterized by SLS first. Due to the higher-order self-association of Rad52, the M value of the wild-type protein is very sensitive to concentration and is not suitable for SLS. The M value for Rad52(218–418) is also concentration-dependent, but less so than wild-type and a narrow concentration range could be studied. A consistent size at low concentrations between 0.2 and 1.2 mg/ml was 102($\pm$25) kDa and corresponded to a trimeric Rad52(218–418) complex (Table 2, row 1). Higher concentrations result in a shift in the M value to 153($\pm$40) kDa equivalent to a tetrameric complex of Rad52(218–418) as was shown previously.[14] The RPA14/32
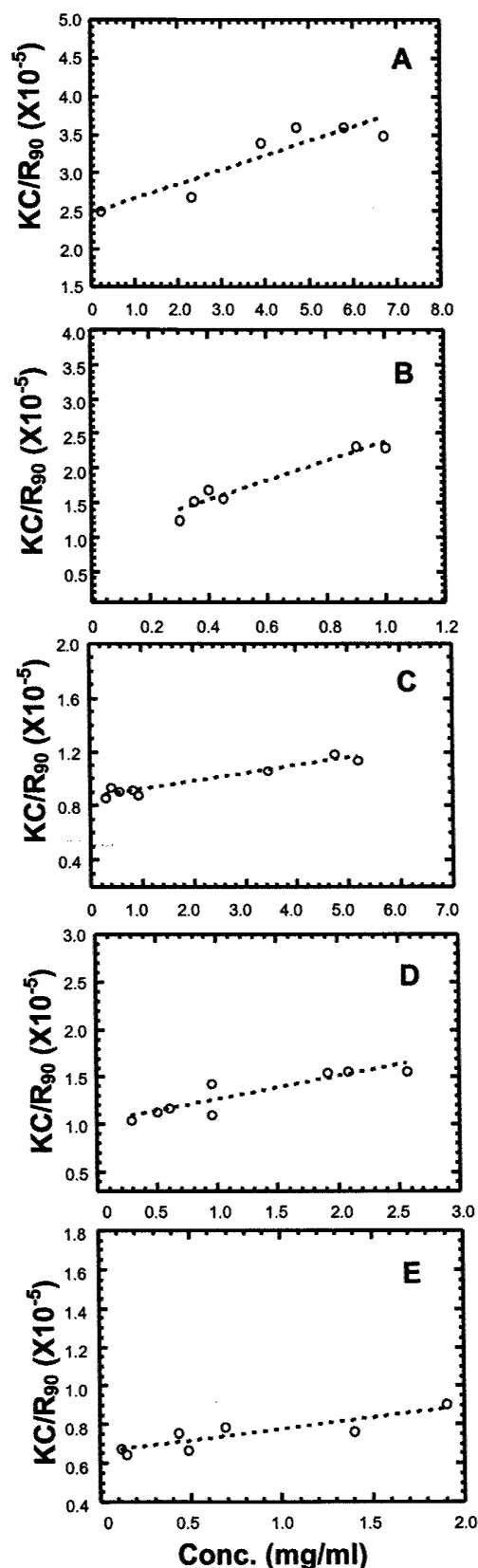
heterodimer alone had an M value of $42(\pm 11)$ kDa, which corresponds to a single heterodimer in solution (Table 2, row 3). Previous studies at three-fold higher protein concentrations indicated a dimer of dimers in solution.[14] SLS measurements of RPA heterotrimer alone show an M value of $117(\pm 11)$ kDa (Table 2, row 2), which is consistent with previous results with the RPA heterotrimer obtained by hydrodynamic analysis and analytical ultracentrifugation.[21,43] These data indicate that these preparations of RPA14/32 and RPA hetero-trimer have equal molar ratios of RPA14, RPA32 and RPA70 subunits.

Complex formation between RPA and Rad52 appears to disrupt the trimeric aggregates of Rad52(218–418). When Rad52(218–418) was added to RPA14/32 and RPA heterotrimer in an equal molar ratio of monomer to heterodimer or heterotrimer, the resulting complexes had M values of $99(\pm 22)$ kDa and $152(\pm 28)$ kDa, respectively (Table 2, rows 4 and 5). The RPA14/32:Rad52 (218–418) and RPA:Rad52(218–418) complexes show an increase in molecular mass of approxi-mately one Rad52(218–418) subunit. There was no increase in the polydispersity, as indicated by the standard deviation of the R_H, upon complex formation. This indicates that aggregates of Rad52(218–418) or free RPA were not detected. These data indicate that the binding of RPA to Rad52(218–418) is very effective at disrupting the higher-order self-association of Rad52.

Discussion

Regions of RPA important for binding Rad52

Two interaction sites on RPA for Rad52 were defined by the ELISA studies on a large number of RPA mutants to include RPA70 residues 168–326 and RPA32 residues 224–270 (Figure 9). Previous work had identified a specific interaction between human Rad52 and RPA and implicated the acidic CTD of RPA32 as the primary binding region for Rad52.[10] The possibility of an interaction between RPA70 and Rad52 had been eliminated because two RPA70 mutants (called p70d293–373 and p70d374–458) studied retained the ability to bind Rad52. Apparently, these deletions did not disrupt the RPA70:Rad52 binding site, which has been found in this work to be located between residues 169 and 382. The relative affinities of the RPA32 and RPA70 sites for Rad52 remain to be determined.

The two interaction sites on RPA for Rad52 are shared by Rad51 and XPA (Figure 9). When the RPA:Rad51 complex was studied by

Figure 8. Static light-scattering data used for the molecular mass determinations summarized in Table 2. (a) RPA14/32, (b) Rad52(218–418), (c) RPA, (d) Rad52(218–418):RPA14/32, (e) Rad52(218–418):RPA. Linear least-squares fitting was performed in Kaleida-Graph and the correlation coefficients are 0.82, 0.92, 0.98, 0.96, and 0.89 for (a)–(e), respectively.

Table 2. Static light scattering data for forms of RPA, Rad52 and RPA:Rad52 complexes

Sample[a]	Conc. range (mg/ml)	R_H[b] (nm)	C_p/R_h[c]	SLS M (kDa)	Error[d] (kDa)	Predicted M (kDa)	Complex[e] size
1. Rad52(218–418)[f]	0.2–1.2	4.71 (1.54)	0.321	102	25	38	2.7
2. RPA	0.1–5.0	5.17 (1.10)	0.203	117	11	110	1.1
3. RPA14/32	0.2–4.0	3.78 (0.93)	0.246	42	11	44	0.96
4. RPA14/32:Rad52(218–418)	0.2–3.0	4.41 (1.34)	0.364	99	22	82	1.2
5. RPA:Rad52(218–418)	0.1–4.0	5.21 (0.98)	0.193	153	28	148	1.0

[a] Samples were mixed on a one RPA heterodimer or heterotrimer to one Rad52 monomer ratio.

[b] Average R_H with standard deviation in parentheses is reported from DynaLS.

[c] The average value of the polydispersity divided by the hydrodynamic radius.

[d] Derived from the reciprocal of the y intercept error (See Figure 8).

[e] Complex size is experimentally determined molecular mass divided by the predicted molecular mass.

[f] The size of Rad52(218–418) has been measured by several methods, including scanning transmission electron microscopy, gel-permeation chromatography and DLS, and ranged from three to four subunits depending on the protein concentration.[14] Due to the propensity of Rad52 to form higher-order complexes, wild-type was excluded from SLS experiments and Rad52(218–418) was kept at low concentrations.

immunoprecipitation a subset of the same RPA mutants were used.[37] The 168–326 region on RPA70 was shown to be important for complex formation with Rad51. A role for RPA32 in the complex was not studied completely, but RPA14/32 was shown to coimmunoprecipitate with Rad51. These results appear to imply a role for RPA32 in binding Rad51 that deserves further study. The regions identified for binding XPA are similar to Rad52 but do not overlap exactly.[41] Also, the XPA interaction with RPA14/32 was substantially lower than heterotrimeric RPA.

It is intriguing that the RPA heterodimer binds as tightly to Rad52 as the RPA heterotrimer. At present, a full explanation of this activity cannot be given but there are two likely explanations for

this observation. The heterodimer may adopt a slightly different conformation when RPA70 is not present that promotes Rad52 binding. For example, the RPA32CTD could be more accessible in the absence of RPA70 and the binding of Rad52 promoted by ease of access to RPA32CTD. Alternatively, the CTDs of two RPA14/32, in a
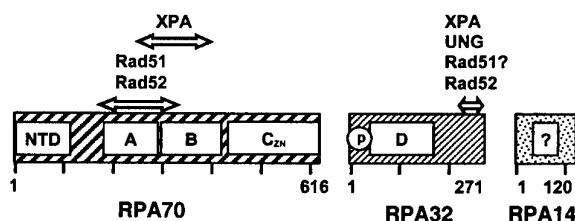

A

```
              uu  u      *u       u
              bbb       bbbb
RPA32(252-267)  EGHIYS---TVDD-DHFKST
              EG|||S  VD| |||||T
RPA70(218-236)  EGKLFSLELVDESGEIRAT
              bbbbbbbbbbb  bbbbbb
              s s         sssss d d
```

B

H. sapiens	EGKLFSLELVDESGEIRAT
D. melanogaster	EGKLFSMDLMDESGEIRAT
S. cerevisiae	DGKLFNVNFLDTSGEIRAT
S. pombe	EGKLFSVNLLDESGEIRAT
X. laevis	EGKLFSIEMVDESGEIRAT

Figure 10. Sequence analysis of the putative binding site for Rad52 on RPA70. (a) In line 1, a u indicates RPA32 residues shown to bind UNG peptide[40] and a * indicates the position of the point mutation D228Y that disrupts Rad52-dependent double-strand break repair in *S. cerevisiae*.[45] In line 2, a b indicates RPA32 residues with β-strand secondary structure. Line 3, the sequence for residues 252–267 of RPA32. Line 4, identical homologous residues between RPA32 and RPA70 are indicated with the amino acid and similar residues are indicated with a vertical line. Lines 5 and 6, the sequence for residues 218–236 of RPA32 and the residues in β-strands are given.[22] Line 7, an s indicates surface-accessible residues and a d indicates residues interacting with ssDNA on RPA70. (b) Peptide sequences of RPA70 residues 218–236 from *Homo sapiens, S. cerevisiae, Schizosaccharomyces pombe, Drosophila melanogaster,* and *Xenopus laevis.* Amino acid residues that are identical with those of *H. sapiens* are in bold. Sequence alignments were performed using the Lipman–Pearson protein alignment available in Lasergene Navigator software (DNASTAR, Inc.) with the following settings: kTuple 2, gap penalty 4 and gap length penalty 6.

Figure 9. Comparison of binding of Rad52, Rad51, XPA and UNG to RPA. Real and putative DNA-binding domains (DBDs) are indicated in boxes as follows. On RPA70: DBD-A, includes residues 181–290; DBD-B, includes residues 300–422; DBD-C$_{ZN}$, includes residues 432–616 and contains a zinc finger; and DBD-NTD, includes residues 1–110. On RPA32: DBD-D, includes residues 43–171.[19,22,23,26,35,47,54] Another OB fold, indicated by a ?, exists on RPA14 that may or may not bind ssDNA.[24] The N terminus of RPA32, which becomes hyperphosphorylated during the cell-cycle and in response to DNA damage, is indicated by a p in a circle. The regions involved in binding Rad52 have been narrowed down to include RPA32 residues 224–271 and RPA70 residues 169–326; Rad51 to include RPA70 residues 169–326 and may possibly involve the C terminus of RPA32;[37] XPA to include RPA32 residues 224–271 and RPA70 residues 236–382;[41] and UNG binds to the RPA32CTD.[55] The regions on Rad52, XPA and UNG thought to bind RPA32CTD share limited homology.[40]

dimer-of-dimers, could closely approximate the surface of the RPA heterotrimer. There is evidence in the literature that RPA14/32 can assemble to form a dimer-of-dimers.[24,44] In this case, two RPA32 CTDs would be bound to Rad52, one in the normal RPA32 site of Rad52 and one in the Rad52 site normally occupied by RPA70. Evidence for the physiological relevance of the heterodimer in apoptosis makes the high affinity of it for Rad52 (and Rad51) even more intriguing.[29,32]

Putative Rad52 binding site on RPA70

We propose that the Rad52 interaction surface on RPA32 and RPA70 are similar in sequence composition. Two pieces of experimental evidence support this proposal. First, the ionic strength data (Figure 7) shows that both of the RPA14/32:Rad52 and RPA70Δ442:Rad52 complexes are disrupted by increasing concentration of salt, which indicates that both interaction surfaces involve electrostatic interactions, also supports this proposal. Secondly, the same region on Rad52 binds RPA14/32 and RPAΔ442 (Figure 5). To further explore this idea, a search for sequence homology was performed between RPA70(169–326) and RPA32(224–271). A homologous, acidic 19 residue peptide, including RPA70 residues 218–236 was found (Figure 10(a)). This putative Rad52 binding surface, RPA70(218–236), is 32% identical with and 79% similar in sequence to RPA32(252–267) and lies completely within DBD-A. This peptide contributes a small acidic patch to the surface of RPA70 and is neighbored by basic residues involved in binding ssDNA.

NMR and X-ray crystallographic structural information is available for the RPA32(252–267) and RPA70(218–236) peptides and is summarized on lines 1, 2, 6 and 7 of Figure 10(a).[22,25,40] The RPA32(252–267) peptide contains a binding surface for UNG2 and XPA, as well as Rad52.[40] In the NMR structure, the side-chains of residues 252, 253, 256, 261 and 267 are involved directly in binding the UNG peptide (line 1, Figure 9(a)) and are well conserved in the RPA70(218–236) peptide (Figure 10(b)). In the crystal structure of RPA70(181–422), the RPA70(218–236) peptide includes a tight turn between two antiparallel β-strands and is near residues involved in DNA binding (line 6, Figure 10(a)).[22,25] Notably, residues 218, 220, 228, 229, 230, and 232 are surface-accessible and are not involved in DNA binding (line 7, Figure 10(a)). DNA-binding residues are nearby and included in this sequence (residues 234 and 236) but their side-chains are mainly positioned on a different tight turn and on the opposite face of the β-sheet than the putative Rad52 binding surface. The 214–217 loop that moves upon DNA binding is just upstream from this sequence.[25] The sequence of the RPA70(218–236) peptide is well conserved (Figure 10(b)). Studies in yeast support the role of the RPA70(218–236) peptide in break repair. In *S. cerevisiae*, the mutation of Asp228 to

Tyr on scRPA70 altered Rad52-dependent DSB repair.[45] This mutation changes an acidic residue to a neutral residue, thereby lowering the electrostatic potential of the surface and possibly changing protein–protein interactions. In summary, the structural homology of the RPA32(252–267) and RPA70(218–236) peptides was not identical, but many secondary structure units are retained and the location on the surface of residues known to be important in protein–protein interactions are strictly conserved. Considering the available data, RPA70(218–236) is proposed to include the binding site for Rad52 on RPA70. Further experimentation will be needed to test this hypothesis.

The involvement of RPA32 in the enhanced ssDNA binding affinity of the RPA:Rad52 complex

The wild-type RPA:Rad52 complex has at least fivefold higher affinity for dT_{30} than RPA alone. In these studies, DNA-binding to a short oligonucleotide 30 residues in length was analyzed. This length corresponds to the occluded binding site size of RPA.[20] Under these conditions, cooperative binding should not occur and only 1:1 RPA:DNA complexes should form. This means that in the RPA:Rad52 complex, Rad52 is probably not interacting with the DNA. This interpretation is supported by the finding that Rad52(218–418), which does not interact with ssDNA but interacts with RPA strongly, enhanced the equilibrium association constant by at least 18-fold. We conclude the effect of Rad52 binding must change the structure of RPA to facilitate higher ssDNA binding. The reason enhancement of Rad52(218–418) is higher than wild-type Rad52 is not known and could be because the ring-forming region of this mutant is missing. Mutations of residues in the OB-fold of RPA32 obliterate this stimulation and thereby support a role for RPA32 in the enhanced binding of ssDNA. Deletion of the RPA32 C-terminal interaction domain for Rad52 also disrupts the increase in affinity. These data indicate that the interaction between RPA and Rad52 is needed to increase the affinity through RPA32. To our knowledge, this is the first example of complex formation increasing the affinity of RPA through the RPA32 subunit. Similar enhancement of RPA ssDNA binding affinity has been seen with the DNA-binding proteins SV40 T-antigen and Gal4/VP16 (K. A. Braun, Y. Lao & M.S.W., unpublished results).[46]

These experiments do not address the effects of Rad52 on cooperative binding of RPA or of binding to long ssDNA lattices. Additional studies will be necessary to determine whether Rad52 stimulates RPA binding under cooperative binding conditions.

Data from a mutational analysis of the relative contribution of the four DNA-binding domains of *S. cerevisiae* RPA to ssDNA-binding affinity

supports the role of RPA32 in binding ssDNA. It showed that DBD-A (in scRPA70) played a primary role in binding short oligonucleotides of 12 nt or less and DBD-D (in scRPA32) interacts with longer oligonucleotides of 27 nt or more.[23] A sequential model of binding was proposed in which DBD-A is responsible for the initial interaction with ssDNA, that domains A, B and C (scRPA70) contact 12–23 nt of ssDNA and that DBD-D (scRPA32) is needed for substrates greater than 23 nt in length. It has been reported that the binding affinity of the RPA14/32 heterodimer is stimulated when the N and C termini of RPA32 were truncated.[47]

Contrary to our initial hypothesis, these data indicate that the stimulation of RPA ssDNA affinity by Rad52 is through ssDNA binding to the RPA32 subunit and not the major ssDNA-binding site in RPA70. This stimulation is mediated by Rad52 binding, is enhanced at higher concentrations of Rad52, and requires that RPA70 be present in the heterotrimer. There are two likely mechanisms to explain these observations. First, the binding of Rad52 to RPA32 may directly open the ssDNA-binding domain within RPA32 (Figure 9, DBD-D). Second, the binding of Rad52 may be affecting the global structure of the heterotrimer and stimulate RPA32 binding in an indirect manner.

Implications for DSB repair mechanism

Three pathways are known to repair double-strand breaks.[1,48] Their relative importance and function between the species is still under investigation. Homologous recombination is thought to be the predominant pathway in *S. cerevisiae*, and non-homologous end-joining as the dominant pathway in humans. Together, RPA and Rad52 can also perform single-strand annealing to repair DSBs in DNA containing repetitive sequences. Homologous recombination has been reconstituted *in vitro* for human and *S. cerevisiae* proteins.[7,8,39] In yeast, the binding of scRad52 is thought to facilitate scRad51 filament formation by displacing scRPA during homologous recombination.[5] The enhanced affinity of the RPA:Rad52 complex for ssDNA indicates that the mechanism of homologous recombination in humans may be different from that in *S. cerevisiae* and it is unlikely that the binding of human Rad52 displaces RPA from ssDNA. On the other hand, the stimulation of RPA ssDNA binding by Rad52 may partly explain the enhanced single-strand annealing seen when RPA is combined with Rad52.[4,6,49] A full understanding of the interplay between ssDNA, RPA, Rad52 and Rad51 binding awaits further experimentation on both human and yeast proteins, including the understanding of the effect protein–protein interactions have on ssDNA binding constants.

Due to the similarities of UNG, XPA and Rad52 in binding RPA, a "hand-off" model has been put forward for the assembly and coordination of different components of the DNA repair machinery.[40] This model suggests that the dynamic assembly of the DNA repair machinery might be organized by multiple, competitive interactions with RPA. Our work contributes three pieces of data that support the hand-off model. First, the binding of Rad52 includes surfaces on both RPA32 and RPA70. Second, similar surfaces on RPA are employed for binding Rad52 and Rad51, that do not overlap completely in surface or activity with XPA (Figure 9). And third, the same surface on Rad52 that binds RPA is involved in the higher-order self-association of Rad52 rings. There is evidence that the higher-order complexes formed by Rad52 are important to its various functions in DSB repair. Rad52 interacts with itself to form heptameric ring complexes and higher-order interactions between ring complexes.[9,12,14] Human Rad52 was shown specifically to bind to DNA ends as an aggregated complex of rings.[12] Rad52 was also shown to facilitate the joining of DNA ends by bacteriophage T4 DNA ligase by Rad52-Rad52 intermolecular interactions.[12] The contribution of the higher-order self-association of Rad52 rings to single-strand annealing of complementary ssDNA ends has been confirmed by EM.[15] Here, we show that these Rad52 intermolecular interactions are disrupted in the presence of RPA, and thus RPA is competing for the same or nearby site on the C terminus of Rad52. The competition between RPA and Rad52 for the Rad52 C-terminal self-association surface may be of importance for the orchestration of the three DSB repair pathways. It was noted that high concentrations of human Rad52 were inhibitory to Rad51-mediated strand-exchange activity.[8,37] It is tempting to speculate that this inhibition was relieved by addition of RPA, perhaps through the displacement of higher-ordered Rad52 ring complexes by RPA binding. In conclusion, dynamic protein–protein and protein–DNA interactions involving complexes of RPA, Rad52 and Rad51 appear to be important component of DSB repair.

Materials and Methods

Generation of Rad52 monoclonal antibodies

Initial injections of 50 μg of wild-type Rad52 in complete Freund's adjuvant were given subcutaneously to eight to nine week old female Balb/C mice. Three additional boosts with 50 μg of antigen were given intraperatoneally without adjuvant at two week intervals. After the final injection, the mice were boosted two additional days and sacrificed by cervical dislocation on the fourth day. Splenocytes were isolated by passage through a wire mesh and red blood cells were removed by incubation with red blood cell lysis buffer (Sigma) on ice for ten minutes. Primary splenocytes were fused with the mouse myeloma cell line P3/NS1/1-Ag4-1 (American Type Culture Collection (ATCC), Rockville, MD.) in the presence of PEG (1300–1600 Da). The complete fusion was plated in 96-well plates and medium containing aminopterin was added the following day to eliminate unfused myeloma cells. Hybridoma

supernatants were screened by Western blot of bacterially expressed Rad52. Positive hybridomas were cloned by limiting dilution to isolate a clonal population of antibody-producing cells. Hybridomas were maintained in HY medium (Sigma) supplemented with 20% (v/v) fetal bovine serum (Hyclone Laboratories, Logan, UT). In total, 64 hybridomas cell lines were isolated. The epitopes of the secreted antibodies were mapped coarsely to the domains of Rad52 by Western blot with wild-type Rad52, Rad52(1–192), Rad52(1–303) and hRad52(1–340). Six antibodies that recognized different domains of Rad52 were identified and used in ELISA and immunoprecipitation.

Generation of Rad52 deletion mutant constructs

Wild-type human Rad52 (pRad52wt), Rad52(1–192), Rad52(1–303), and Rad52(1–340) pET28 expression plasmids, each with six histidine residues on the C terminus, were a gift from Dr M. Park (Los Alamos National Laboratories). Rad52(218–418) was prepared by amplifying the specific coding region of the wild-type gene in pRad52wt. The N-terminal PCR primer was: 5′-CAGCTGCAGCAGGTGACCTCCCCTTCC-3′ and the C-terminal PCR primer was 5′-GTGG-CCTGgaatTCAGTtAGATGGAT-3′, which contained an engineered unique downstream *Eco*RI restriction site after the stop codon (underlined). PCR was performed using Taq polymerase (Promega) in a DNA thermal cycler (Perkin Elmer) using standard conditions. The PCR product was cloned into a pBAD/Thio-TOPO fusion vector (INVITROGEN) by TA-TOPO cloning. This ligation creates a fused thioredoxin gene N-terminal to the Rad52(218–418) gene sequence. The fusion protein gene sequence was then amplified from the pBAD/Thio-TOPO fusion vector using oligonucleotides: upstream 5′-CCGACCGcAtATGGCCCTGGGACACC-3′ and the same downstream primer. The upstream primer contained the upstream thioredoxin start sequence and an engineered *Nde*I site. The sequence was ligated into the *Nde*I site and *Eco*RI site of a pET28 vector. The resulting fusion protein contained an N-terminal His$_6$ tag preceding a thioredoxin tag sequence and the Rad52(218–418) gene sequence.

Protein purification

Wild-type and mutant Rad52 were expressed and purified under reducing conditions as described.[14] The Rad52(218–418) purification was modified to include dialysis into 50 mM Caps (pH 10.2), 1 M KCl, 2% (v/v) glycerol, 0.5 mM *n*-hexyl-glucoside, 1 mM DTT, 1 mM EDTA and then loaded onto a Superdex 200 gel-filtration column. The eluted protein was stored in this buffer. Wild-type and mutant RPA were purified as described.[19,44,50,51] Protein concentrations were determined by the Bradford method using BSA as a standard. The concentrations of RPA, RPA 14/32, and Rad52(218–418) were corrected using extinction coefficients of 8.44×10^4, 2.34×10^4 and 3.41×10^4 at 280 nm from precipitated protein denatured with GuHCl. For Rad52(218–418) practically identical concentrations were given by both methods. For RPA, A_{280} gave 1.2-fold lower concentrations.

Protein complexes were formed for static and dynamic light-scattering by adding equal molar amounts of RPA or RPA14/32 with Rad52(218–418) in a 15 ml micro-concentrator (Centricon-50). The protein solutions were diluted ≥ 20-fold in Rad52/RPA binding buffer (50 mM Hepes (pH 7.8), 150 mM KCl, 2% glycerol, 0.5 mM *n*-hexylglucoside, 1 mM DTT, 1 mM EDTA). Then the proteins were concentrated at 4 °C for 8–12 hours at 500 g and to allow complexes to form.

Enzyme-linked immunosorbant assay (ELISA)

The ELISA was performed as described.[14,35] The substrates used were (2′2′-azinobis[3-ethylbenzothiozoline-6-sulfonic acid] (ABTS), 3,3′,5,5′ tetramethyl benzidine(TMP) or *o*-phenylenediame (OPD) in phosphate buffer and 0.01% (v/v) hydrogen peroxide. For ABTS, the absorbance was monitored at 405 nm. For TMP and OPD, the absorbance at 450 nm was monitored.

In order to study the effect of salt on the RPA:Rad52 complexes, a slightly modified ELISA protocol was used where the second protein (RPA) was diluted with a range of different concentrations of salt before it was allowed to interact with Rad52. This interaction step was followed by a wash step before detection of bound RPA with antibody.

Immunoprecipitation

Purified RPA (10 pmol of either wild-type RPA or RPA32Δ224) was mixed with 20 pmol of Rad52 in a 6 μl reaction volume containing HM buffer (30 mM Hepes (pH 7.8), 0.5% (w/v) inositol, 0.01% (v/v) NP40, 1 mM DTT, 5 mM MgCl$_2$) at room temperature for one hour. Each reaction was immunoprecipitated with 300 μl of anti-Rad52 hybridoma conditioned supernatant and rocked at 4 °C for 30 minutes. Then 50 μg of anti-mouse affinity gel (ICN) was added to the antibody–antigen complex and the reaction rocked at 4 °C for 30 minutes. The beads were spun down and washed five times with TBST buffer (10 mM Tris–HCl (pH 8.0), 150 mM NaCl, 0.05% (v/v) Tween-20). Samples were separated by SDS-PAGE (8% polyacrylamide gel) and transferred to nitrocellulose. The nitrocellulose was cut horizontally at approximately 60 kDa. The top half was immunoblotted using a monoclonal antibody to RPA70 (Calbiochem). The bottom half was probed for histidine-tagged Rad52 with INDIA probe (Pierce) and visualized by chemiluminescence. Initial characterization by Western analysis using wild-type and mutant Rad52 allowed rough mapping of their epitopes: mAb1 and mAb2 mapped to residues 1–192, mAb3 to residues 193–303, mAb4 to residues 304–340, and mAb5 and mAb6 to residues 341–418 (Figure 1). To further characterize the Rad52 antibodies, the ability of any of the antibodies to disrupt the RPA:Rad52 interaction was explored by immunoprecipitation. In immunoprecipitation reactions, all six anti-Rad52 antibodies pull down the RPA:Rad52 complex and RPA32ΔC224 complex equivalently.

Gel mobility-shift assay (GMSA)

Gel mobility-shift assays were performed as described but with slight modifications.[18,21] Binding assays were carried out in 15 μl volume in FBB buffer (30 mM Hepes (diluted from 1 M stock at pH 7.8), 100 mM NaCl, 5 mM MgCl$_2$, 0.5% inositol, 1 mM DTT). The indicated amount of protein(s) was then incubated with 2 fmol of radio-labeled dT$_{30}$ and 50 μg/ml of BSA at 25 °C for 20 minutes. When protein mixtures were used, the proteins were premixed and incubated on ice for ten minutes prior to being added to the reaction mixtures Reactions

were then brought to a final concentration of 4% glycerol, 0.01% (w/v) bromophenol blue and electrophoresed on a 1% (w/v) agarose gel in 0.1 × TAE buffer. The gels were then dried on DE81 paper and radioactive bands were visualized by autoradiography. The radioactivity in each band was quantified using a Packard Instant Imager. Binding isotherms were obtained by plotting the fraction of oligonucleotide remaining unbound *versus* RPA concentration. Intrinsic binding constants were determined by non-linear least-squares fitting the data to the Langmuir binding equation (KaleidaGraph-Synergy Software) as described.[18,21]

Surface plasmon resonance (SPR)

Interaction of RPA, Rad52 or mutants with ssDNA was monitored using a surface plasmon resonance (SPR) biosensor instrument, Biacore 3000 (Biacore). The 5′-biotinylated dT30 DNA was diluted to 64 nM in a buffer containing 10 mM sodium acetate (pH 4.8), 1 M NaCl and injected manually onto an immobilized streptavadin surface of the BIAcore sensor chip SA to the desired density in different flow-cells. One flow-cell was left underivatized to allow for refractive index change correction. Proteins were diluted in the running buffer containing 10 mM Hepes (pH 7.4), 1 M NaCl, 2 mM MgCl$_2$, 0.005% (w/v) polysorbate-20, 1 mM DTT. Protein was injected into the ssDNA surface (30RU) using the kinject function of Biacore. Association phase was allowed for 600 seconds followed by 400 seconds of buffer injection period for dissociation. Following RPA and Rad52 binding, regeneration was performed with a quick injection of 100 mM NaOH. Data were analyzed using a simple Langmuir 1:1 model.

Static and dynamic light-scattering

Dynamic light-scattering (DLS) was carried out using a DynaPro-801 molecular sizing instrument equipped with a microsampler (Protein Solutions). The instrument has a laser wavelength of 828.7 nm and a fixed scattering angle of 90°. DLS is based on the collected autocorrelation function of the scattered intensity. The acquisition time for all experiments was ten seconds. A 50 μl sample was passed through the filtering assembly into a 12 μl chamber quartz cuvette. All proteins were filtered with 20 nm filters (Whatman). The data were analyzed first with the Dynamics 4.0 software and then the DynaLS software. These gave consistent values for the hydrodynamic radius (R_H) and polydispersity (C_p). All distributions were monomodal, meaning a single distribution of molecules, for this study as defined by the baseline values range from 0.997–1.002. The sum of squares (SOS) error represents the error in the decay of the autocorrelation function. Good SOS errors are 5% or less. The resolution slider values were optimized by the DynaLS software. The resolution slider value represents the maximum allowable information about the distribution without including effects of noise.

Each of the static light-scattering (SLS) data points, at various concentrations, represents a single DLS experiment. The average intensity for approximately 25–30 data points (30–45 minutes) at a 90° angle was measured. This average intensity for each protein concentration was used to calculate Rayleigh ratios with toluene as the reference solvent. The SLS by a protein depends on the concentration, the scattered light

intensity, and the molecular mass as follows:[52]

$$\frac{KC}{R_{90}} = \frac{1}{M} + 2B_{22}C$$

where C is the protein concentration, R_{90} is the Rayleigh ratio at 90°, B_{22} is the second virial coefficient, M is the average molecular mass of the protein in solution, and K is the optical constant. Since the particles under study are more than ten times smaller than the wavelength, the shape of the particles does not need to be considered.

$$K = \frac{1}{N_A} \left(\frac{2\pi n_o}{\lambda^2} \right)^2 \left(\frac{dn}{dC} \right)^2$$

where N_A is Avogadro's number, λ is the wavelength, n_o is the refractive index of the solution and dn/dC is the refractive index increment of the protein solution with protein concentration. The value for dn/dC used here was 0.186 ml/g. The Raleigh ratio (KC/R_{90}) is plotted *versus* protein concentration and fit by linear regression. The molecular mass was obtained from the y intercept. The error was estimated from the linear least-squares fit to the data (KaleidaGraph). Sources of errors include intensity fluctuations and protein concentration measurements. All data points for SLS were monomodal distributions with SOS errors near 5% or below. For every SLS experiment, R_H was monitored and the differences due to higher concentration or aggregation were less than 5% of R_H. It was not possible to perform SLS experiments on wild-type Rad52 because of its significant dependence on R_H with concentration.[14]

References

1. Shinohara, A. & Ogawa, T. (1995). Homologous recombination and the roles of double-strand breaks. *Trends Biochem. Sci.* **20**, 387–391.
2. Sung, P. (1997). Function of yeast Rad52 protein as a mediator between replication protein A and the Rad51 recombinase. *J. Biol. Chem.* **272**, 28194–28197.
3. Benson, F. E., Baumann, P. & West, S. C. (1998). Synergistic actions of Rad51 and Rad52 in recombination and DNA repair. *Nature*, **391**, 401–404.
4. Shinohara, A., Shinohara, M., Ohta, T., Matsuda, S. & Ogawa, T. (1998). Rad52 forms ring structures and cooperates with RPA in single-strand DNA annealing. *Genes Cells*, **3**, 145–156.
5. New, J. H., Sugiyama, T., Zaitseva, E. & Kowalczykowski, S. C. (1998). Rad52 protein stimulates DNA strand exchange by Rad51 and replication protein A. *Nature*, **391**, 407–410.

6. Sugiyama, T., New, J. H. & Kowalczykowski, S. C. (1998). DNA annealing by RAD52 protein is stimulated by specific interaction with the complex of replication protein A and single-stranded DNA. *Proc. Natl Acad. Sci. USA*, **95**, 6049–6054.

7. McIlwraith, M. J., Dyck, E. V., Masson, J.-Y., Stasiak, A. Z., Stasiak, A. & West, S. C. (2000). Reconstitution of the strand invasion step of double-strand break repair using human Rad51 Rad52 and RPA proteins. *J. Mol. Biol.* **304**, 151–164.

8. Baumann, P. & West, S. C. (1999). Heteroduplex formation by human Rad52 protein effects of DNA end-structure, hRPA and hRad52. *J. Mol. Biol.* **291**, 363–374.

9. Van Dyck, E., Hajibagheri, N. M. A., Stasiak, A. & West, S. C. (1998). Visualisation of human Rad52 protein and its complexes with hRad51 and DNA. *J. Mol. Biol.* **284**, 1027–1038.

10. Park, M. S., Ludwig, D. L., Stigger, E. & Lee, S. H. (1996). Physical interaction between human RAD52 and RPA is required for homologous recombination in mammalian cells. *J. Biol. Chem.* **271**, 18996–19000.

11. Kagawa, W., Kurumizaka, H., Ikawa, S., Yokoyama, S. & Shibata, T. (2001). Homologous pairing promoted by the human Rad52 protein. *J. Biol. Chem.* **276**, 35201–35208.

12. Van Dyck, E., Stasiak, A. Z., Stasiak, A. & West, S. C. (1999). Binding of double-strand breaks in DNA by human Rad52 protein. *Nature*, **398**, 728–731.

13. Stasiak, A. Z., Larquet, E., Stasiak, A., Muller, S., Engel, A., Dyck, E. V. *et al.* (2000). The human Rad52 protein exists as a heptameric ring. *Curr. Biol.* **10**, 337–340.

14. Ranatunga, W., Jackson, D., Lloyd, J. A., Forget, A. L., Knight, K. L. & Borgstahl, G. E. O. (2001). Human Rad52 exhibits two modes of self-association. *J. Biol. Chem.* **276**, 15876–15880.

15. Dyck, E. V., Stasiak, A. Z., Stasiak, A. & West, S. C. (2001). Visualization of recombination intermediates produced by RAD52-mediated single-strand annealing. *EMBO Rep.* **2**, 905–909.

16. Wold, M. S. (1997). RPA: a heterotrimeric single-stranded DNA-binding protein required for eukaryotic DNA metabolism. *Annu. Rev. Biochem.* **66**, 61–91.

17. Iftode, C., Daniely, Y. & Borowiec, J. A. (1999). Replication protein A (RPA): the eukaryotic SSB. *Crit. Rev. Biochem. Mol. Biol.* **34**, 141–180.

18. Kim, C., Snyder, R. O. & Wold, M. S. (1992). Binding properties of replication protein A from human and yeast cells. *Mol. Cell. Biol.* **12**, 3050–3059.

19. Gomes, X. V., Henricksen, L. A. & Wold, M. S. (1996). Proteolytic mapping of human replication protein A: evidence for multiple structural domains and a conformational change upon interaction with single-stranded DNA. *Biochemistry*, **35**, 5587–5594.

20. Gomes, X. V. & Wold, M. S. (1996). Functional domains of the 70-kilodalton subunit of human replication protein A. *Biochemistry*, **35**, 10558–10568.

21. Kim, C., Paulus, B. F. & Wold, M. S. (1994). Interactions of human replication protein A with oligonucleotides. *Biochemistry*, **33**, 14197–14206.

22. Bochkarev, A., Pfuetzner, R. A., Edwards, A. M. & Frappier, L. (1997). Crystal structure of the DNA binding domain of replication protein A bound to DNA. *Nature*, **385**, 176–181.

23. Bastin-Shanower, S. A. & Brill, S. J. (2001). Functional analysis of the four DNA binding domains of replication protein A: the role of RPA2 in ssDNA binding. *J. Biol. Chem.* **276**, 36446–36453.

24. Bochkarev, A., Bochkareva, E., Frappier, L. & Edwards, A. M. (1999). The crystal structure of the complex of replication protein A subunits RPA32 and RPA14 reveals a mechanism for single-stranded DNA binding. *EMBO J.* **18**, 4498–4504.

25. Bochkareva, E., Belegu, V., Korolev, S. & Bochkarev, A. (2001). Structure of the major single-stranded DNA-binding domain of replication protein A suggests a dynamic mechanism for DNA binding. *EMBO J.* **20**, 612–618.

26. Jacobs, D. M., Lipton, A. S., Isern, N. G., Daughdrill, G. W., Lowry, D. F., Gomes, X. & Wold, M. S. (1999). Human replication protein A: global fold of the N-terminal RPA-70 domain reveals a basic cleft and felxible C-terminal linker. *J. Biomol. NMR*, **14**, 321–331.

27. Blackwell, L., Borowiec, J. & Mastrangelo, I. (1996). Single-stranded DNA binding alters human replication protein A structure and facilitates interaction with DNA-dependent protein kinase. *Mol. Cell. Biol.* **16**, 4798–4807.

28. Din, S.-U., Brill, S. J., Fairman, M. P. & Stillman, B. (1990). Cell cycle regulated phosphorylation of DNA replication factor A from human and yeast cells. *Genes Dev.* **4**, 968–977.

29. Treuner, K., Okuyama, A., Knippers, R. & Fackelmayer, F. O. (1999). Hyperphosphorylation of replication protein A middle subunit (RPA32) in apoptosis. *Nucl. Acids Res.* **27**, 1499–1504.

30. Rodrigo, G., Roumagnac, S., Wold, M. S., Salles, B. & Calsou, P. (2000). DNA replication but not nucleotide excision repair is required for UVC-induced replication protein A phosphorylation in mammalian cells. *Mol. Cell. Biol.* **20**, 2696–2705.

31. Henricksen, L. A., Carter, T., Dutta, A. & Wold, M. S. (1996). Phosphorylation of human replication protein A by the DNA-dependent protein kinase is involved in the modulation of DNA replication. *Nucl. Acids Res.* **24**, 3107–3112.

32. Treuner, K., Findeisen, M., Strausfeld, U. & Knippers, R. (1999). Phosphorylation of replication protein A middle subunit (RPA32) leads to a disassembly of the RPA heterotrimer. *J. Biol. Chem.* **274**, 15556–15561.

33. Loo, Y.-M. & Melendy, T. (2000). The majority of human replication protein A remains complexed throughout the cell cycle. *Nucl. Acids Res.* **28**, 3354–3360.

34. Dimitrova, D. S. & Gilbert, D. M. (2000). Stability and nuclear distribution of mammalian replication protein A heterotrimeric complex. *Expt. Cell Res.* **254**, 321–327.

35. Braun, K. A., Lao, Y., He, Z., Ingles, C. J. & Wold, M. S. (1997). Role of protein–protein interactions in the function of replication protein A (RPA): RPA modulates the activity of DNA polymerase α by multiple mechanisms. *Biochemistry*, **36**, 8443–8454.

36. Stigger, E., Drissi, R. & Lee, S. H. (1998). Functional analysis of human replication protein A in nucleotide excision repair. *J. Biol. Chem.* **273**, 9337–9343.

37. Golub, E. I., Gupta, R. C., Haaf, T., Wold, M. S. & Radding, C. M. (1998). Interaction of human RAD51 recombination protein with single-stranded DNA binding protein, RPA. *Nucl. Acids Res.* **26**, 5388–5393.

38. Hays, S. L., Firmenich, A. A., Massey, P., Banerjee, R. & Berg, P. (1998). Studies of the interaction between Rad52 protein and the yeast single-stranded DNA binding protein RPA. *Mol. Cell. Biol.* **18**, 4400–4406.

39. Song, B. W. & Sung, P. (2000). Functional interactions among yeast Rad51 recombinase, Rad52 mediator,

and replication protein A in DNA strand exchange. *J. Biol. Chem.* **275**, 15895–15904.

40. Mer, G., Bochkarev, A., Gupta, R., Bochkareva, E., Frappier, L., Ingles, C. J. *et al.* (2000). Structural basis for the recognition of DNA repair proteins UNG2, XPA and Rad52 by replication factor RPA. *Cell,* **103**, 449–456.

41. Walther, A. P., Gomes, X. V., Lao, Y., Lee, C. G. & Wold, M. S. (1999). Replication protein A interactions with DNA. 1. Functions of the DNA-binding and zinc-finger domains of the 70-kDa subunit. *Biochemistry,* **38**, 3963–3973.

42. Lao, Y. (2001). Multiple interactions between DNA and human replication protein A (RPA). PhD Dissertation, University of Iowa, Department of Biochemistry, Iowa City, IA.

43. Sibenaller, Z. A., Sorensen, B. R. & Wold, M. S. (1998). The 32- and 14-kilodalton subunits of replication protein A are responsible for species-specific interactions with single-stranded DNA. *Biochemistry,* **37**, 12496–12506.

44. Habel, J. E., Ohren, J. F. & Borgstahl, G. E. O. (2001). Dynamic light scattering analysis of full-length, human RPA14/32 dimer: purification, crystallization and self-association. *Acta Crystallog. sect. D,* **D57**, 254–259.

45. Smith, J. & Rothstein, R. (1999). An allele of *RFA1* suppresses RAD52-dependent double-strand break repair in *Saccharomyces cerevisiae. Genetics,* **151**, 447–458.

46. Lao, Y., Gomes, X. V., Ren, Y., Taylor, J. S. & Wold, M. S. (2000). Replication protein A interactions with DNA. III. Molecular basis of recognition of damaged DNA. *Biochemistry,* **39**, 850–859.

47. Bochkareva, E., Frappier, L., Edwards, A. M. & Bochkarev, A. (1998). The RPA32 subunit of human replication protein A contains a single-stranded DNA-binding domain. *J. Biol. Chem.* **273**, 3932–3936.

48. Haber, J. E. (1999). Gatekeepers of recombination. *Nature,* **398**, 665–667.

49. Mortensen, U. H., Bendixen, C., Sunjevaric, I. & Rothstein, R. (1996). DNA strand annealing is promoted by the yeast Rad52 protein. *Proc. Natl Acad. Sci. USA,* **93**, 10729–10734.

50. Henricksen, L. A., Umbricht, C. B. & Wold, M. S. (1994). Recombinant replication protein A: expression, complex formation and function characterization. *J. Biol. Chem.* **269**, 11121–11132.

51. Gomes, X. V. & Wold, M. S. (1995). Structural analysis of human replication protein A; mapping functional domains of the 70-kDa subunit. *J. Biol. Chem.* **270**, 4534–4543.

52. Kratochvil, P. (1987). *Classical Light Scattering from Polymer Solutions,* Elsevier, Amsterdam.

53. Shen, Z., Peterson, S. R., Comeaux, J. C., Zastrow, D., Moyzis, R. K., Bradbury, E. M. & Chen, D. J. (1996). Self-association of human RAD52 protein. *Mutat. Res.* **364**, 81–89.

54. Pfuetzner, R. A., Bochkarev, A., Edwards, A. M. & Frappier, L. (1997). Replication protein A: characterization and crystallization of the DNA binding domain. *J. Biol. Chem.* **272**, 430–434.

55. Nagelhus, T. A., Haug, T., Singh, K., Keshav, K. F., Skorpen, F., Otterlei, M. *et al.* (1997). A Sequence in the N-terminal region of human uracil-DNA glycosylase with homology to XPA interacts with the C-terminal part of the 34-kDa subunit of replication protein A. *J. Biol. Chem.* **272**, 6561–6566.